Nat. Hazards Earth Syst. Sci. Discuss., https://doi.org/10.5194/nhess-2018-186
Manuscript under review for journal Nat. Hazards Earth Syst. Sci.
Discussion started: 27 August 2018

Natural Hazards and Earth System Sciences
Open Access
Discussions

Landsliding near Enguri dam (Caucasus, Georgia) and possible seismotectonic effects

Alessandro Tibaldi [1], Paolo Oppizzi [2], John Gierke [3], Thomas Oommen [3], Nino Tsereteli [4], Davit Odilavadze [4]

[1] University of Milan Bicocca, Milan, Italy
[2] Geolog, Chiasso, Switzerland
[3] Michigan Technological University, Houghton, USA
[4] M. Nodia Institute of Geophysics, M. Javakhishvili Tbilisi State University, Georgia

Correspondence to: Alessandro Tibaldi (alessandro.tibaldi@unimib.it)

Abstract. The Enguri dam and water reservoir, nested in southwestern Caucasus (Republic of Georgia), are surrounded by steep mountain slopes. At a distance of 2.5 km from the dam, a mountain ridge along the reservoir is affected by active deformations with a double vergence. The western slope, directly facing the reservoir, has deformations that involve a subaerial area of 1.2 km^2. The head scarp interests the main Jvari-Khaishi-Mestia road with offset of man-made features that indicate slip rates of 2-9 cm/y. Static, pseudostatic and Newmark numerical analyses, based on field and seismological data, suggest different unstable rock volumes basing on the environment conditions. An important effect of variation of water table is showed, as well as the possible destabilization of the landslide following seismic shaking compatible with the expected local Peak Ground Acceleration. This worst scenario corresponds to an unstable volume in the order of up to $48 \pm 12*10^6$ m^3. The opposite, eastern slope of the same mountain ridge is also affected by wide deformation involving an area of 0.37 km^2. Here, field data indicate 2-5 cm/y of short-term and long-term slip rates. Ground Penetrating Radar surveys of the head scarps confirm that these slip planes are steep and extend downward. All these evidences are interpreted as resulting from two similar landslides, whose possible causes are discussed, comprising seismic triggering, mountain rapid uplift, river erosion and lake variations.

Key words: Caucasus, slope deformation, seismicity, Enguri dam

1 Introduction

GPS data and plate tectonic models indicate that the Greater and Lesser Caucasus are tectonically very active, with ongoing mountain building processes comprising complex deformation with vertical and horizontal strain partitioning (Rebai et al., 1993; Koçyiğit et al., 2001; Reilinger et al., 1997, 2006; Tan and Taymaz, 2006; Pasquaré et al., 2011). These processes result from the still developing convergence and continent-continent collision between the Eurasian and Africa-Arabian plates (Avagyan et al., 2010; Adamia et al., 2017) (Fig. 1). The active deformation is accompanied by diffuse seismicity that reaches M_s of 6-7 (Tsereteli et al., 2016) and Intensity up to 10 (Varazanashvili et al., 2018) in the Caucasus in the Republic of Georgia.

In the southwestern part of the Georgian Greater Caucasus, there is the Enguri dam (the World's sixth highest dam) (Fig. 2A) that is part of the Enguri hydroelectric power station. This facility is the main hydroelectric plant of Georgia that presently furnishes the major part of the energy to the country. The Enguri dam is located nearby a series of geological features that suggest Quaternary uplift, comprising deeply-entrenched rivers, deformed river terraces, recent faults and folds, and very steep slopes (Tibaldi and Tsereteli, 2017; Tibaldi et al., 2017a). The strategic importance of the Enguri hydroelectric plant and the fact that it is nested within one of the most tectonically active regions of Caucasus, suggest the necessity of carrying out modern studies on the stability of the slopes surrounding the 19-km-long water reservoir, which are completely missing in the scientific literature (only one technical consultant report exists, which is unpublished - CGS, 2015). Mountain slopes, in fact are subject to gravity effects that can be enhanced by earthquake shaking (Gutierrez-Santolalla et al., 2005); it has been widely demonstrated that this shaking can cause generation of shallow landslides and deep-seated gravity slope deformations (DSGSDs) in active seismic areas (Beck, 1968; Solonenko, 1977; McCleary et al., 1978; Radbruch-Hall, 1978; Tibaldi et al., 1995; McCalpin, 1999). The dynamic loading produced by seismicity may trigger discrete episodes of fast slope deformation (e.g. Beck, 1968) or may accelerate already existing movements along DSGSD structures (e.g. Pasuto and Soldati, 1996). Whether the movements are continuous (Varnes et al., 1989, 1990, 2000) or intermittent (Beget, 1985), the slopes under active deformation pose a threat to infrastructures (Mahr, 1977; Radbruch-Hall, 1978; McCalpin and Irvine, 1995). Nearby the Enguri reservoir there is also the important main road connecting the famous town of Mestia, hosting several ancient monuments and a sky resort, with the rest of Georgia. This road is affected by important slope deformations in correspondence of the same slope that faces the Enguri water reservoir. Moreover, in general, slope movements can turn into dangerous catastrophic collapses, examples of which have been reported in Japan (Chigira and Kiho, 1994), Italy (Semenza and Ghirotti, 2000) and Canada (Evans and Couture, 2002).

The present paper aims to describe, for the first time, the main active slope deformations affecting a mountain ridge that runs along the eastern side of the Enguri water reservoir. The approach is multidisciplinary since it comprises geological, geomorphological, structural and georadar surveys, completed with local seismic Peak Ground Acceleration calculation and numerical modelling of slope instability. The focus is to give the main first evidence that allows to define the boundaries of the unstable slopes, their geometries, kinematics, slip rate and volume. Field observations are completed by preliminary 2-D numerical static, pseudostatic and dynamic modelling. 3-D modelling requires further extensive work that will be carried out in the future and deserves a proper publication. The results show the presence of wide active slope deformations that interest the two opposite slopes of this mountain ridge.

The paper has a series of main international impacts: i) it describes an outstanding example of intense gravity instability with double vergence, ii) it contributes to answer to the challenging scientific questions on the causes that can increase the instability of a slope facing a reservoir, and iii) it elucidates the regional processes that can contribute to induce intense slope instability. The paper also iv) represents a contribution to assess the hydrogeologic hazard of the largest hydroelectrical facility of Georgia.

Nat. Hazards Earth Syst. Sci. Discuss., https://doi.org/10.5194/nhess-2018-186
Manuscript under review for journal Nat. Hazards Earth Syst. Sci.
Discussion started: 27 August 2018

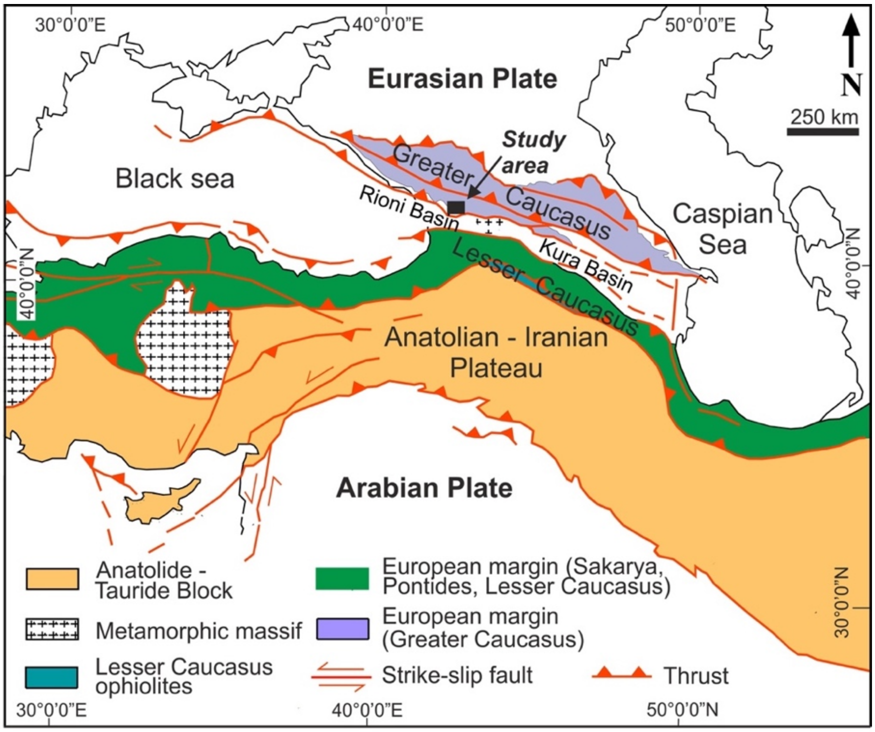

Figure 1: Tectonic map of the Arabia - Eurasia collision zone (modified from Sosson et al., 2010).

2 Geological background

The Greater and Lesser Caucasus are two fold-and-thrust belts separated by the Black Sea - Rioni basin and the South Caspian - Kura intermontane depression (Fig. 1) (Adamia et al., 1977, 2010; Banks et al., 1997; Mosar et al., 2010; Sosson et al., 2010). The Rioni and Kura regions first developed as foreland basins, in Oligocene-Early Miocene times, and successively were involved in the fold-and-thrust belts, representing an example of intra-plate, fast-growing mountain building process in Neogene times (Forte et al., 2010; Adamia et al., 2011; Alania et al., 2016). Fault-bend folds and fault-propagation folds are widespread with evidence of thin-skinned tectonics in both the Rioni and Kura fold-and-thrust belts (Adamia et al., 2010; Forte et al., 2010; Alania et al., 2016). Intense deformation involved these belts during the last 14-15 Ma, characterized by important fault slip along the main thrust systems that reached the greatest rate at the end of the Miocene (Adamia et al., 2017; Alania et al., 2016). These structural data are coherent with the results of apatite fission-track studies that revealed that the greatest exhumation rate occurred in the Miocene-Pliocene in the Greater Caucasus, although starting here in the Oligocene (Avdeev and Niemi, 2011; Vincent et al., 2007, 2011).

Successively, the mountain building processes continued up to the Quaternary as testified by geodetic and seismic data (Tsereteli et al., 2016). More in detail, historical and instrumental catalogues, seismic reflection sections, focal mechanism solutions, and field geological-structural surveys, show the presence of active compressional tectonics both in the core of the

Nat. Hazards Earth Syst. Sci. Discuss., https://doi.org/10.5194/nhess-2018-186
Manuscript under review for journal Nat. Hazards Earth Syst. Sci.
Discussion started: 27 August 2018

Greater Caucasus as well as along the southern border and at the fold-and-trust belts (Tsereteli et al., 2016; Tibaldi et al., 2017a, 2017b). These authors showed that in the core of the Greater Caucasus there is a series of active reverse faults that are parallel to the mountain range (i.e. WNW-ESE). They dip mostly towards NNE and display pure dip-slips. Along the southern front of the Greater Caucasus, where the Enguri dam is located, there is a zone of active thrusting along planes dipping towards NNE. The Transcaucasus depression, located between the Greater and Lesser Caucasus, shows active inversion tectonics at part of the Rioni Basin with uplift, folding, and faults mostly hidden under the youngest sedimentary cover (Tibaldi et al., 2017a, 2017b). The largest instrumental and historical earthquakes, with M_s 6-7, occurred both in the core of the two mountain belts and along their fronts. Hypocenters are mostly located at depths < 30 km, with depths increasing eastward. A detailed new assessment of historical earthquakes of all Georgia, assigns Intensity values up to 10 to the Caucasus region (Varazanashvili et al., 2018). These data are consistent with geodetic observations by Reilinger et al. (2006), which indicate a total convergence rate of 2-3 cm/y between the plates located south and north of the Caucasus. The same authors suggest that about 1/3 of this convergence is accommodated along the Caucasus by crustal shortening. The total post-collisional sub-horizontal shortening of this mountain belt caused by the northward motions of the Africa-Arabian plate is estimated at hundreds of kilometers (Barrier and Vrielynk, 2008; Meijers et al., 2013).

From a stratigraphic and lithological point of view, pre-Mesozoic basement and Jurassic sedimentary rocks characterize the axial zone of the Greater Caucasus, whereas Cretaceous and Cenozoic sedimentary rocks are present in the more external zones (Adamia et al., 2011; Mosar et al., 2010). At the foot of the southwestern Greater Caucasus, where the Enguri dam is located, carbonatic deposits dominate together with rarer terrigenous and tuffaceous rocks of volcanic origin. More detailed data on the local geology are given below.

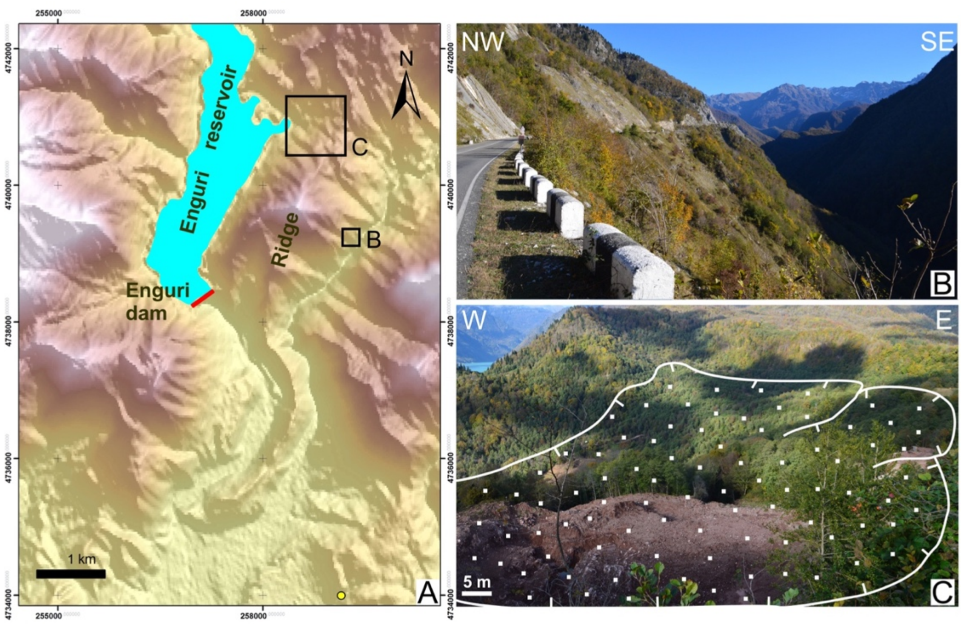

Nat. Hazards Earth Syst. Sci. Discuss., https://doi.org/10.5194/nhess-2018-186
Manuscript under review for journal Nat. Hazards Earth Syst. Sci.
Discussion started: 27 August 2018

Figure 2: A. DEM of the Enguri dam area. Boxes locate Figures 2B and 2C. B. Segment of the Jvari-Khaishi-Mestia road where it crosses the eastern slope of the ridge highlighted in Figure 2A; here rocks and slopes are very steep, up to 70°. C. Oblique view (looking north) of the area, facing the Enguri water reservoir, affected by active slope deformation. The scale is referred only to the forefront zone.

3 Results

3.1 Local geology and geomorphology

The studied area shows the presence of Jurassic volcanic and terrigenous rocks and Cretaceous carbonatic deposits generally dipping to the south (Fig. 3). Cretaceous strata crop out around the Enguri dam where they dip mostly at 60-70° (Fig. 2B), whereas they become steeper southward, assuming a vertical dip near the Rioni plain, accompanied by local overturning of the strata with a steep dip to the north. Strata assume a gentler inclination northward, becoming up to subhorizontal towards the northern part of the Enguri reservoir. The region is affected by faults and folds that make the structural architecture locally more complicated. North of the Enguri dam, below the carbonatic strata, there are also Jurassic deposits made of sandstones, tuffs, tuff-breccia and gypsum layers that locally crop out along the southeastern side of the artificial water reservoir (Fig. 3). Their dip is again dominantly towards southeast and south, and generally becomes gentler northward, in the order of 15-40°.

From a geomorphological point of view, the studied area is characterised by the presence of two parallel river valleys trending about N-S (Fig. 2A). The western valley hosts the Enguri dam, whereas the eastern valley is deeply entrenched with differences of altitudes between the valley bottom and the mountain ridge up to 700 m. These two valleys are separated by an about 9-km-long mountain ridge whose western slope constitutes the side of the artificial water reservoir. The two opposite slopes of the mountain ridge are very steep, reaching up locally an inclination of 70° linked with the presence of outcropping carbonatic rocks steeply dipping southward. The Jvari-Khaishi-Mestia main road runs along this mountain ridge and is under the threat of small landslides and, especially, of rolling stones at several sites, in particular where the road comes across the outcropping steep rock strata (Fig. 2B).

Nat. Hazards Earth Syst. Sci. Discuss., https://doi.org/10.5194/nhess-2018-186
Manuscript under review for journal Nat. Hazards Earth Syst. Sci.
Discussion started: 27 August 2018

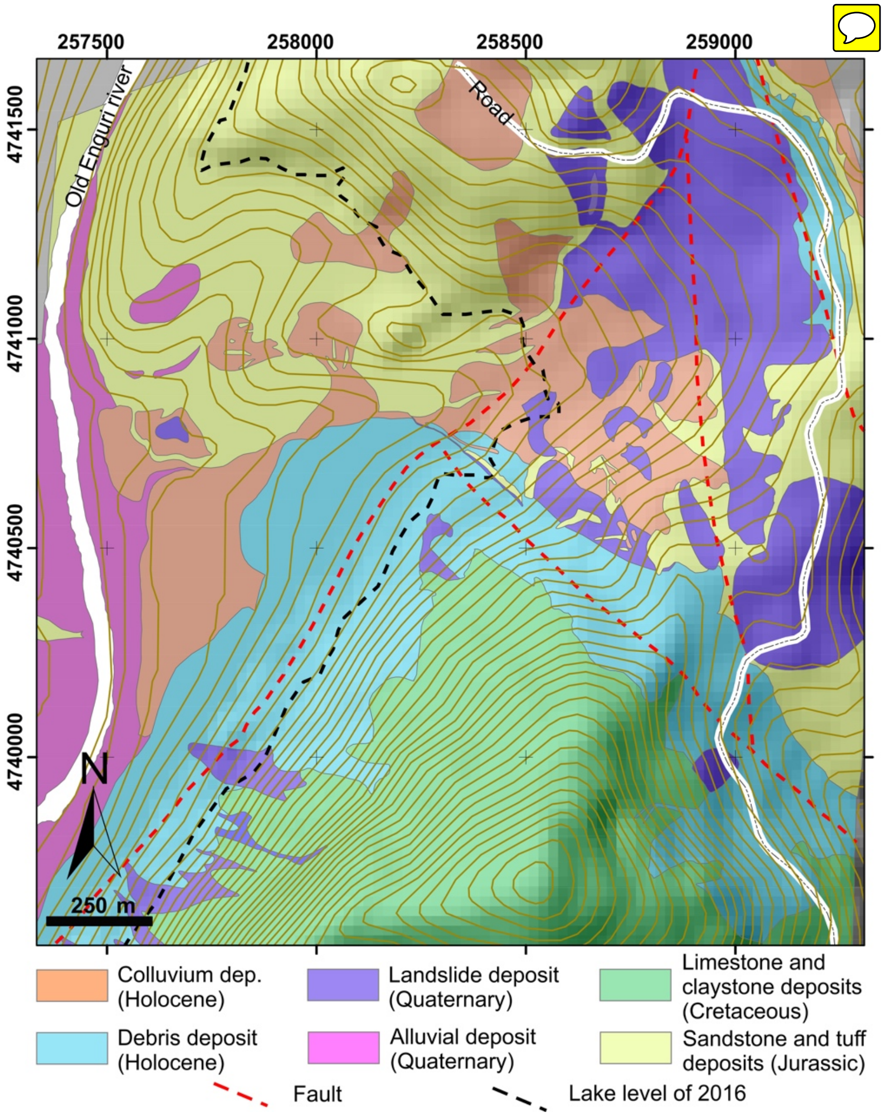

Figure 3: Geological map of the area surrounding the western landslide, based on our new field surveys in the onshore zone and data from Zolotarev et al. (1968) for the zone now submerged by the Enguri water reservoir.

Nat. Hazards Earth Syst. Sci. Discuss., https://doi.org/10.5194/nhess-2018-186
Manuscript under review for journal Nat. Hazards Earth Syst. Sci.
Discussion started: 27 August 2018

Natural Hazards and Earth System Sciences
Open Access
Discussions

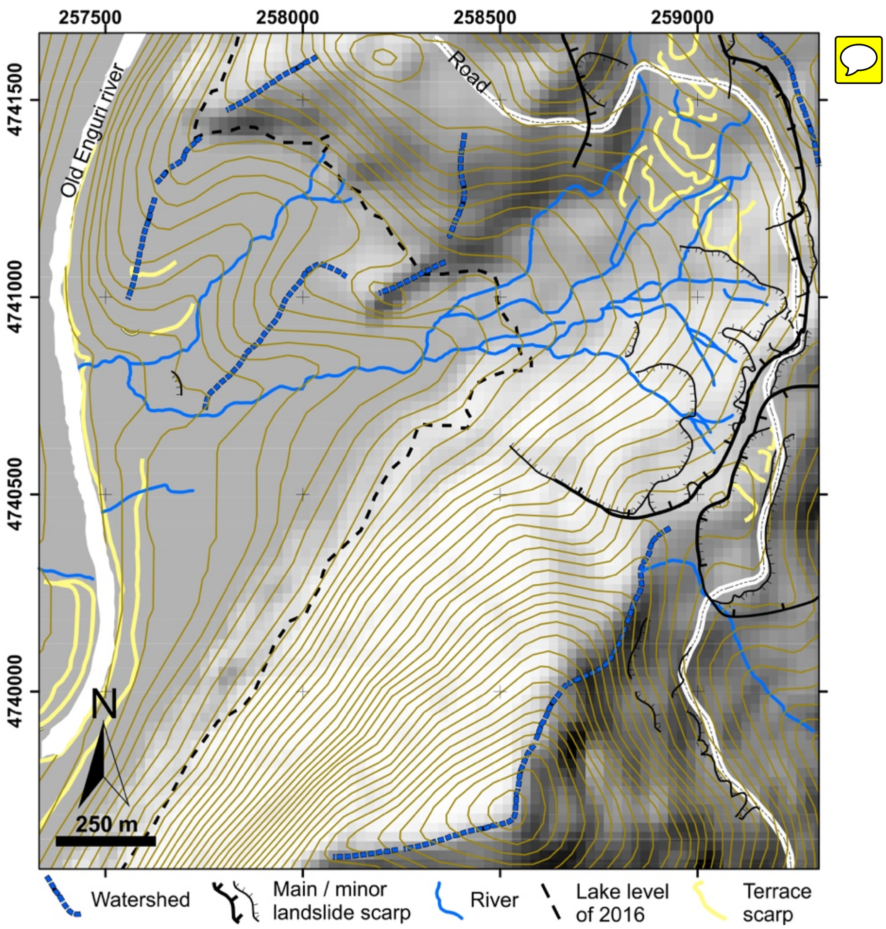

Figure 4: Geomorphological map of the area surrounding the western landslide, based on our new field surveys in the onshore zone and data from Zolotarev et al. (1968) for the zone now submerged by the Enguri water reservoir.

3.2 Morphostructural field evidence of the western landslide

The western slope of the mountain ridge faces directly the Enguri water reservoir. At a distance of about 2.5 km from the Enguri dam, this slope shows a series of landforms typical of recent/active deformation: along the Jvari-Khaishi-Mestia road, at an altitude of 720-740 m, there is a series of scarps facing westward (Figs. 2C and 4). They have a sinuous shape in plan view, given by anastomosed single scarps with a westward concave side. This suggests that these features resulted from joining a series of discrete head scarps. Each scarp is from a minimum of 20 m up to 70 m high. At the scarp foot, the slope is from sub-horizontal to gentle dipping westward (average inclination = 17°), whereas several changes of inclination are present along the slope. These changes are highlighted as terrace scarps in Figure 4: they have been checked in the field and do not correspond to man-made features. Most of these scarps are oriented perpendicularly to the local slope dip and are located in the upper part of the slope. These data suggest they may represent secondary ruptures within a moving slope. This is further confirmed by the presence of several tilted trees, with local zones where 100% of trunks are tilted, all along the area highlighted in Figure 2C.

In regard to river streams, they have been outlined based on the present network and topographic maps surveyed before the formation of the water reservoir. Rivers mostly run along the average slope dip down to about half of the original slope with a dendritic pattern (Fig. 4). At the lower half of the slope, now completely covered by the lake, one single river was draining the landslide area. A few river anomalies are present: at the foot of the slope, now under the lake, the lowermost segment of the aforementioned single river was running parallel to the main Enguri river but with a northward flow. In the northern, upper part of the slope affected by the landslide, one short river segment runs perpendicular to the average slope dip. These river diversions may correspond to anomalies in the average slope topography.

In regards to fractures and fissures, these affect all the area close to the head scarps. The asphalted surface of the Jvari-Khaishi-Mestia road, here is affected by several offsets: deformation is represented by fissures, up to a few cms wide, and scarps facing westwards (Fig. 5). These structures are parallel to sub-parallel to the morphological head scarps. The scarps offsetting the road have been repeatedly measured from November 2015 to May 2017, showing a vertical component of offset up to 14 cm developed during this time frame, giving an average slip rate of 9.3 cm/y at the northernmost, fastest structure. As an example, in Fig. 5B we report the northern scarp surveyed on November 2015, that was 11 cm high; the same scarp then increased to 20 cm in May 2016 (Fig. 5C).

In the southern segment of the head scarps, a detailed survey in the forest showed the presence of tens of meters long, and up to 3.8 m wide fissures (e.g. Fig. 5D). All the fissures are vegetated and mostly filled, with local presence of trees grown inside the fissure, with trunks of about 20 cm in diameter. The bottom of the fissures is filled by coarse debris and soil, while the empty upper part of the fissures has a depth in the range of 1-3 m. This suggests that these fissures have a long history, at least of some tens of years. The area at the foot of this fissure swarm is locally known as Khoko landslide. Presently, gypsum is here excavated at a small open mine for economic reasons (Fig. 5A). At the foot of this landslide, nearby the coast of the artificial water reservoir, we recognized the presence of intensely deformed gypsum rocks (Fig. 5E).

We opened two trenches across some of the main active scarps affecting the Jvari-Khaishi-Mestia road (Fig. 6). The trenches show evidence of repeated downthrown of the western block. The western part of Trench 1, in fact, contains two buried old road surfaces: the oldest is lowered of 1.3 m respect to the present road level, whereas the second one is lowered of 20 cm (Fig. 6C). Interviews with local inhabitants indicated that the oldest road was made during the Soviet era, about AD 1960 ± 5 ys. Although we are aware that the Soviet road was narrower than the present one, the presence of filling material between the various road levels indicates that subsidence here did occur since it was necessary to restore the road plane level. Also at nowadays, in fact, continuous road maintenance is here necessary with tens of centimeters of asphalt added above the downhill segment of the road surface to maintain the level. Trench 2 also contains two buried roads, plus a level of collapsed trees and pieces of woods that is offset by several slip planes dipping downslope (Fig. 6D).

The total subaerial area affected by slope deformation is of 1.2 km^2. The slip surface is not unique and probably there are different, partially superimposed slip planes as suggested by the complexity of the head scarps and of slope morphology, and

Nat. Hazards Earth Syst. Sci. Discuss., https://doi.org/10.5194/nhess-2018-186
Manuscript under review for journal Nat. Hazards Earth Syst. Sci.
Discussion started: 27 August 2018

the dimension of the whole unstable slope. All the piezometers installed during 2015 across the landslide body, are broken at depths between 16 and 49 m, as can be appreciated by comparing columns 6th and 8th in Table 2. These widespread ruptures should correspond to the depth of some active slip planes. Other logs anyway, drilled during the Soviet era (see the section on numerical modelling), suggest that the intact substrate rock is located at deeper levels. This can be seen, for example, in the logs n. 3261 and 3297 (drilled in 1966) (Fig. 7). These logs show the presence of clastic, unconsolidated deposits, rich in clay and locally gypsum fragments, down to a depth of 57.5 m (log 3297), and/or clastic deposits with a sill to clay matrix down to at least 61 m (log 3297) and at least 80 m (log 3261). Other logs, such as n. 3291 (drilled in 1966), indicate clay and gypsum deposits down to a depth of 30 m, below which there is the substrate. These observations, together with detailed geological and geomorphological surveys, allowed to prepare the geological vertical section shown in Figure 7B, which in turn is the base to construct the geotechnical section used for numerical modelling of slope stability. The geological section indicates that the intact substrate rock is located at a variable level, always deeper than 30 m and locally even > 80 m.

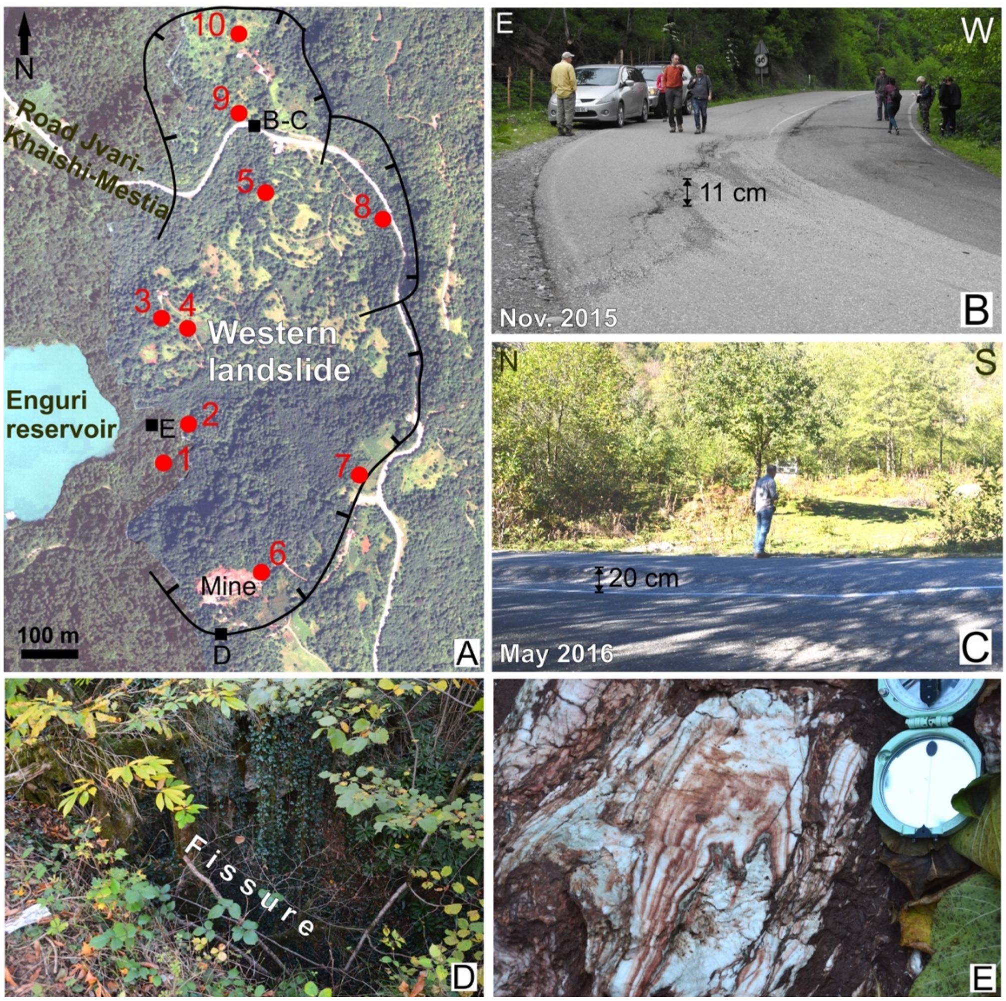

Nat. Hazards Earth Syst. Sci. Discuss., https://doi.org/10.5194/nhess-2018-186
Manuscript under review for journal Nat. Hazards Earth Syst. Sci.
Discussion started: 27 August 2018

Natural Hazards and Earth System Sciences
Open Access
EGU
Discussions

Figure 5: A. Black lines show the main head scarps of the unstable slope area facing the Enguri reservoir. Black boxes locate Figures B-E. Red dots are location of piezometers discussed in the modelling section. B. and C. Photos of one of the several slip planes that offset the Jvari-Khaishi-Mestia road, taken in November 2015 and May 2016 respectively; note the large increase of offset. D. NE-SW-striking fissure located at the head scarp of the southern part of the unstable slope area. E. Strongly deformed gypsum deposits located at the foot of the northern part of the unstable slope area.

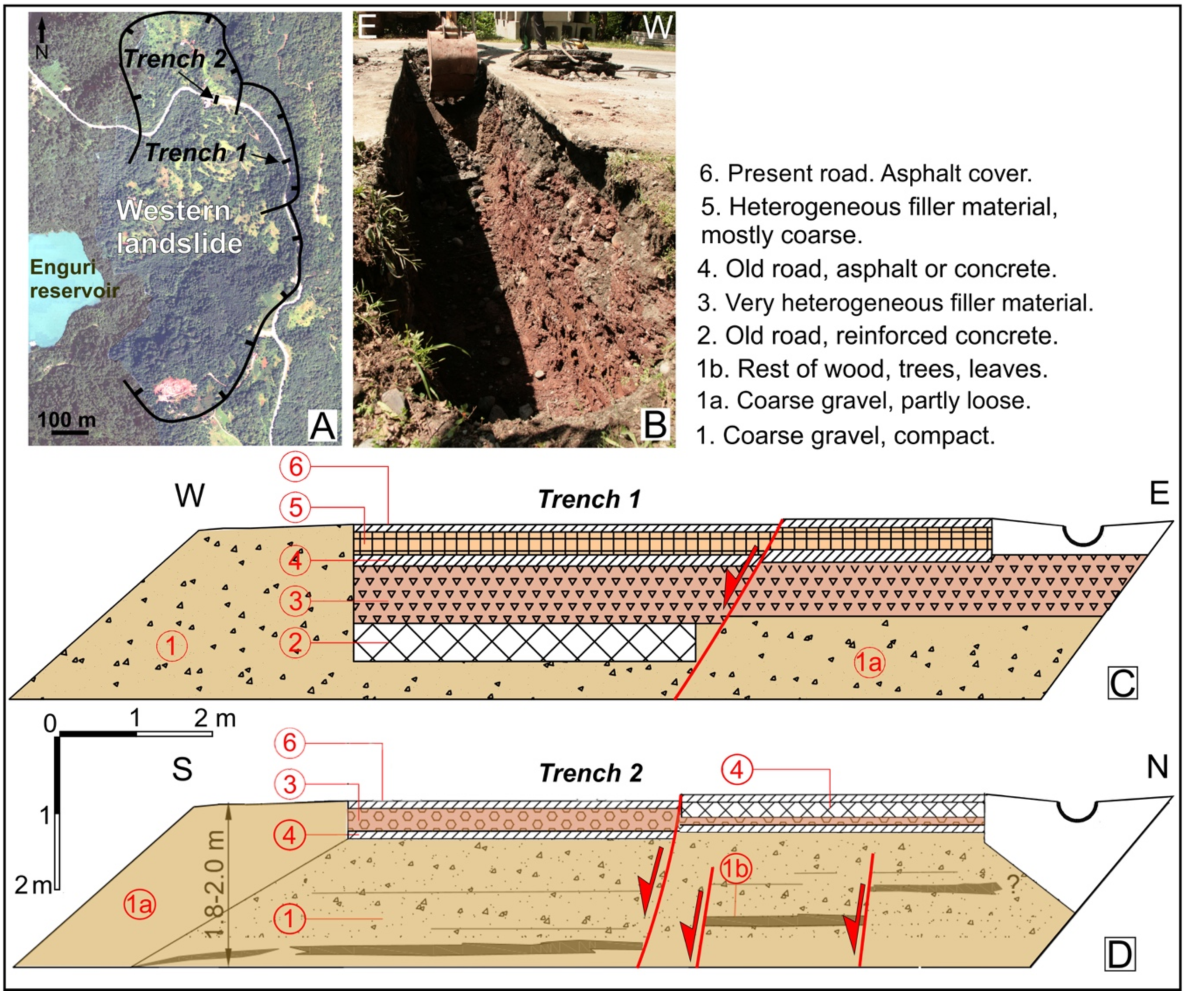

Figure 6: A. Location of the trenches at the northern part of the unstable slope facing the Enguri reservoir. B. Photo of Trench 2 opened across one of the main active scarps affecting the Jvari-Khaishi-Mestia road, location in Figure 6A. C. and D. Logs of the northern and western wall of Trench 1 and 2, respectively. Numbers refer to the legend. Present and old, offset roads are white. The oldest road is downthrown to the west of 1.3 m. The red lines show the location of shallow active slip planes.

Nat. Hazards Earth Syst. Sci. Discuss., https://doi.org/10.5194/nhess-2018-186
Manuscript under review for journal Nat. Hazards Earth Syst. Sci.
Discussion started: 27 August 2018

Natural Hazards and Earth System Sciences
Open Access
Discussions

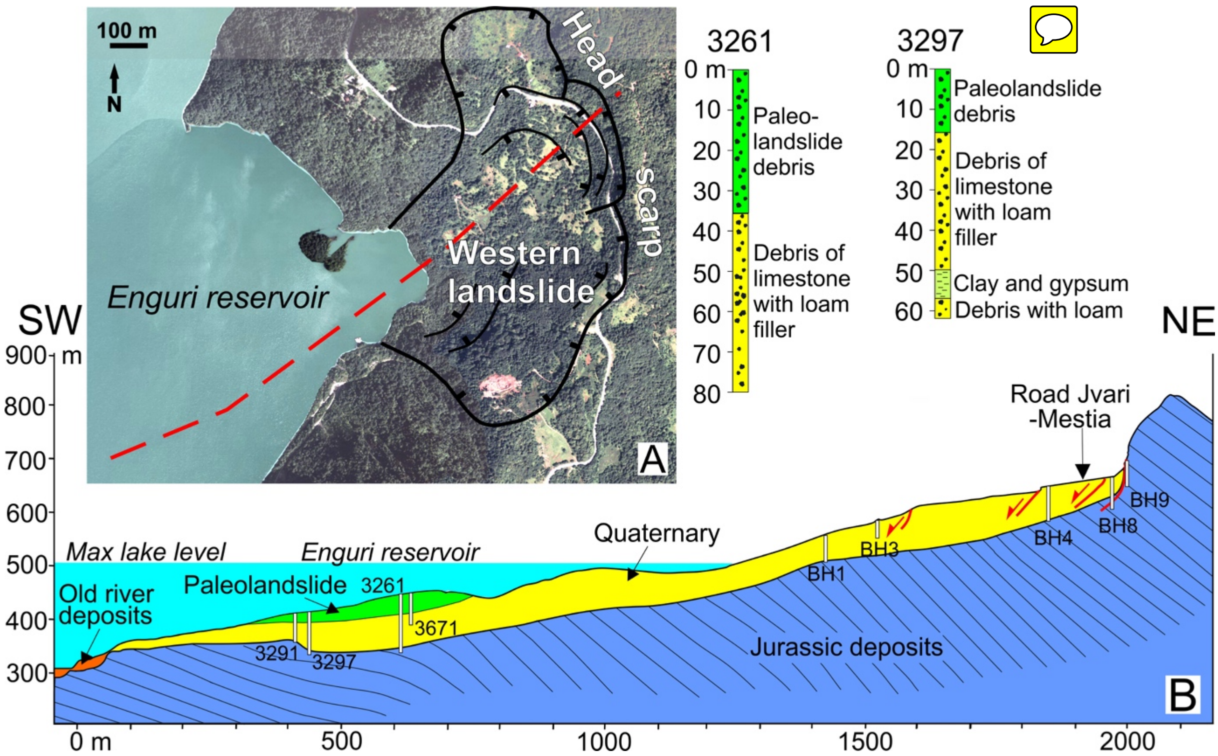

Figure 7: A. Trace (red line) and B. geological section across the slope facing the Enguri reservoir. White columns represent locations and depth of logs used to construct the cross section. Data of the submerged part derived from geological surveys made at the Soviet era before dam construction. Two examples of detailed logs (3261 and 3297) are given.

3.3 Field evidence of the eastern landslide

Also the east-facing slope of the same mountain ridge described above, is affected by active deformations (Figs. 8A and 9). Here, the Jvari-Khaishi-Mestia road, at an altitude of 715-720 m, is characterized by a series of fractures with two main orientations: one set is parallel to the road, that is to say follows the topographic contour lines with a N-S strike. The other fracture set strikes about E-W, perpendicular to the slope.

Most N-S-striking fractures show evidence of extension, with horizontal and vertical offsets of several cm of the road surface. The N-S fractures follow an escarpment that runs along part of this east-facing slope for a total length of about 450 m. At the southern end of this escarpment, the road has deformations with lower amounts of offset.

The fractures striking E-W show dominant left-lateral strike-slip motions in the order of several cm of the road surface (e.g. Fig. 8B). A secondary, local extensional (vertical) component is also present. The resulting net slip indicates left-lateral

Nat. Hazards Earth Syst. Sci. Discuss., https://doi.org/10.5194/nhess-2018-186
Manuscript under review for journal Nat. Hazards Earth Syst. Sci.
Discussion started: 27 August 2018

transtensional motions. An old, N-S trending concrete wall, located along the head scarp, is tilted of 5° towards north (Figs. 8C-D). It is also left-laterally offset by 190 cm, as measured in November 2015, and 195 cm, as measured in may 2017 (Fig. 8E). Nearby, a recent road water channel was also left-laterally offset by 5 cm during a November 2015 measurement (Fig. 8F), which increased to 7 cm in may 2017. These offset man-made features are aligned with an offset white strip painted on the asphalt of the Jvari-Khaishi-Mestia road (Fig. 8B). The white strip shows a left-lateral offset of 8 cm. Interviews with local inhabitants and authorities gave indication of an age of AD 1974 for the concrete wall, whereas the white strips were painted two years before we got the offset data.

The total area affected by slope deformation is of 0.37 km^2. In this area, the lacking of drillings did not allow to assess the possible depth of the main slip surface. A simple projection of the possible depth of potential slip surfaces allowed to speculate about a possible range of volume of the total unstable mass of $40 \pm 7*10^6$ m^3. Anyway, we wish to stress that this estimate must be confirmed by further studies.

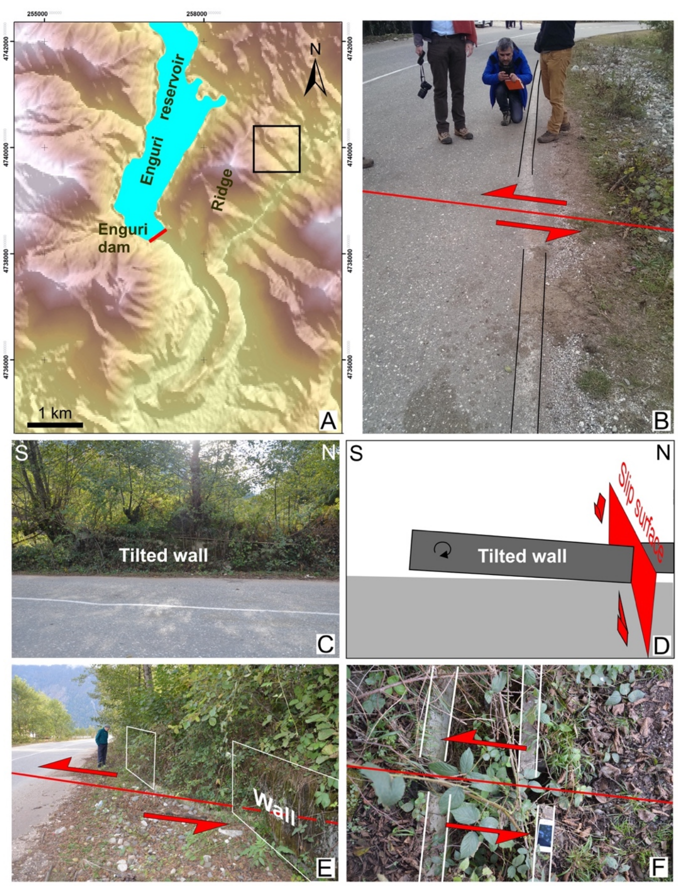

Figure 8: Features observed at the eastern landslide, located in the box of Figure A. B. Left-lateral offset of the Jvari-Khaishi-Mestia road white strip. C. and D. Photo and interpretation of the tilted wall along the same road. E. Left-lateral offset of 1.9 m of a 1974 AD wall. F. Left-lateral offset of a recent water channel.

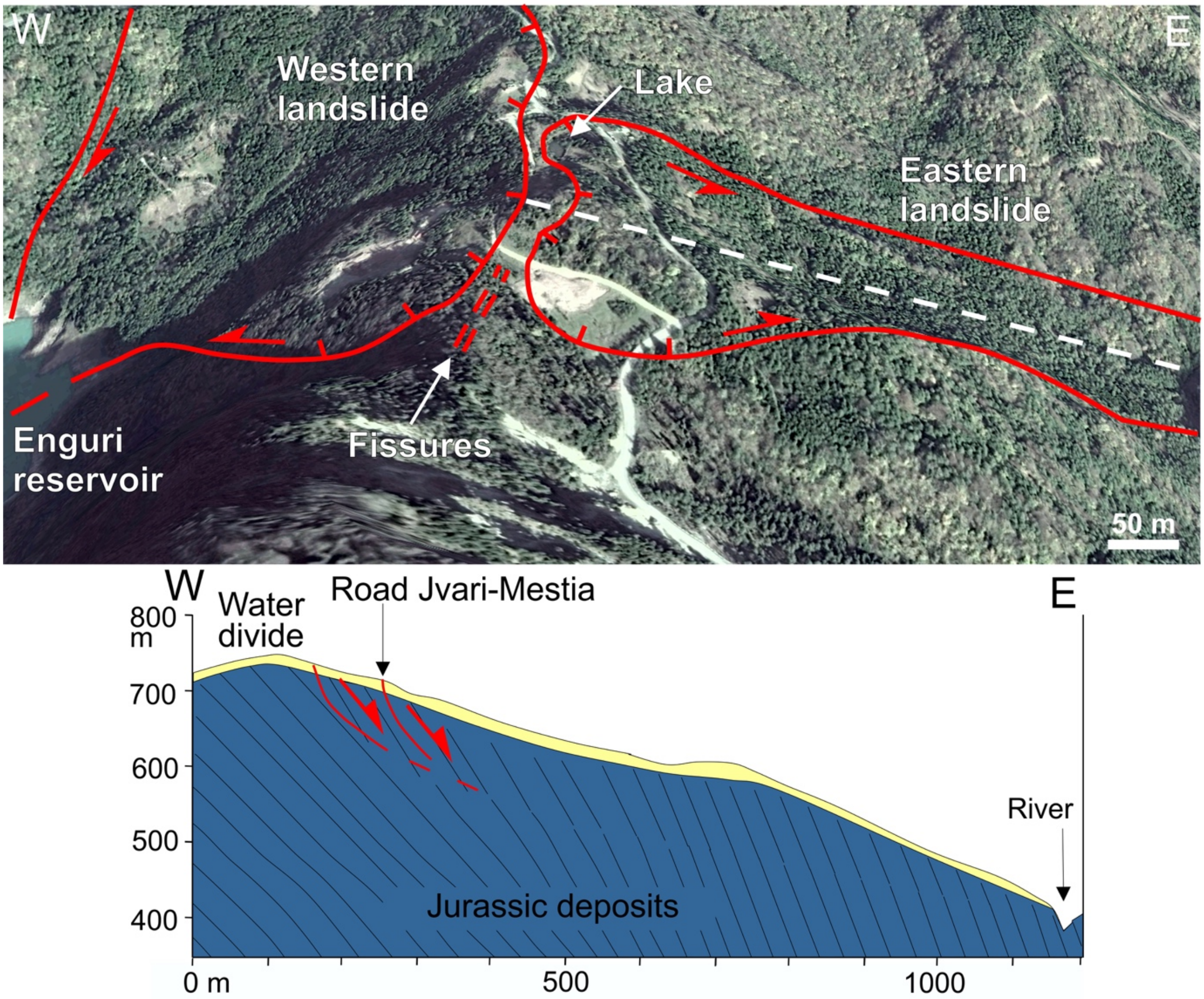

Figure 9: Above: location of the main boundary scarps of the two landslides. Note the small lake at the foot of the head scarp of the eastern landslide, and the fissures located between the head scarps of the two landslides (oblique view from Google Earth). Below: geological section along the eastern landslide, trace is given by the dashed white line in the figure above.

3.4 Georadar surveys

We used a georadar to explore the subsoil of the deformations detected on the surface. Due to the dense forest and steep slopes, the survey was conducted along the Jvari-Khaishi-Mestia road where it intercepts the two landslides. The georadar surveys were conducted using a Zond-12e Ground Penetrating Radar (GPR) equipment, which is a portable digital subsurface sounding radar that can be carried by a single operator. In the surveying process, the operator is getting real-time information

Nat. Hazards Earth Syst. Sci. Discuss., https://doi.org/10.5194/nhess-2018-186
Manuscript under review for journal Nat. Hazards Earth Syst. Sci.
Discussion started: 27 August 2018

comprising a GPS radiolocation profile. The GPR instrument works at single channel or double channel, in the time range from 1 to 2000 ns with 1 ns step. Frequency of pulse repetition of transmitter is 115 KHz with scan rate of 56 (for single channel system) or 80 (for double channel system). We used three different frequencies of the receiver-transmit antenna of 100, 300 and 500 MHz, some examples of which are shown in Figures 10 and 11. The surveys carried out at higher frequencies have good detail only in the very first meters of depth, whereas at lower frequencies the depth of investigation increases but with lower resolution.

Starting with the eastern landslide, a GPR 350-m-long survey has been carried out in a N-S sense along the road, intercepting several slip planes that deform the asphalt, and the main head scarp (Fig. 10A). In the section corresponding to 500 MHz (Fig. 10B), it is possible to observe several vertical to subvertical interruptions of the uppermost strata continuity. At these interruptions, strata show offsets of tens of centimeters, mostly on the southern block. Some of the discontinuities dip steeply southward, corresponding to a normal kinematics due to downsagging of the hangingwall block. Some strata at the northern (right) part of the section are tilted northward, in correspondence of the northernmost detected slip plane. This slip plane coincides in position with the northernmost main landslide slip surface. Its local southward dip and opposite tilting (i.e. northward) of strata are thus coherent with the border position of the structure. In the southern part of the section, strata are tilted southward. The GPR section corresponding to 300 MHz (Fig. 10C) shows the presence of the same discontinuities recognized in the 500 MHz section, indicating they really correspond to slip planes of the landslide that prolong at depth.

At the western landslide, it has been possible to carry out a GPR profile across one of the several active scarps affecting the Jvari-Khaishi-Mestia road (Fig. 11A). The profile trends E-W and is 14-m-long. In the section corresponding to 500 MHz (Fig. 11B), a zone of deformation is visible in the first meter of depth, which separates a dominion to the right (i.e. to the east) of undeformed horizontal strata with respect to a western dominion characterized by tilted strata. Resolution is not enough to observe offset of single strata, but the location of this vertical discontinuity coincides with the slip plane observed on the asphalt. In the 300 MHz and 100 MHz sections, a clear zone of offset strata is recognizable (Figs. 11C-D). Strata are tilted and downsagged, with offsets of tens of centimeters. Downsagged strata are located on the western block, with the slip plane steeply dipping westward, corresponding to a normal kinematics of the hangingwall block. This slip plane coincides in position with the plane of the 500 MHz section and the scarp surveyed in the field.

Nat. Hazards Earth Syst. Sci. Discuss., https://doi.org/10.5194/nhess-2018-186
Manuscript under review for journal Nat. Hazards Earth Syst. Sci.
Discussion started: 27 August 2018

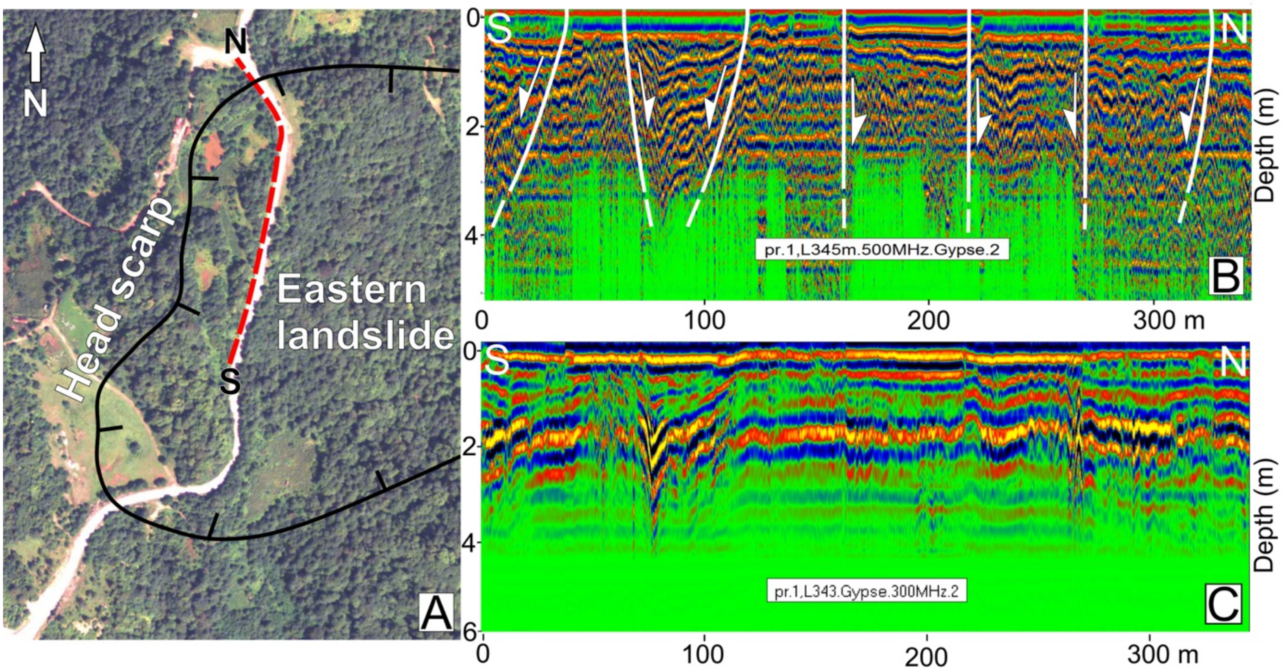

Figure 10: A. Location of the Ground Penetrating Radar (GPR) survey (red dashed line) carried out in the eastern landslide across several active slip planes affecting the main road. The black line shows the uppermost main head scarp of the landslide. GPR sections surveyed with an antenna at: B. 500 MHz, and C. 300 MHz. The 500 MHz section is interpreted with the main slip zones (white lines).

Nat. Hazards Earth Syst. Sci. Discuss., https://doi.org/10.5194/nhess-2018-186
Manuscript under review for journal Nat. Hazards Earth Syst. Sci.
Discussion started: 27 August 2018

Natural Hazards and Earth System Sciences
Open Access
Discussions

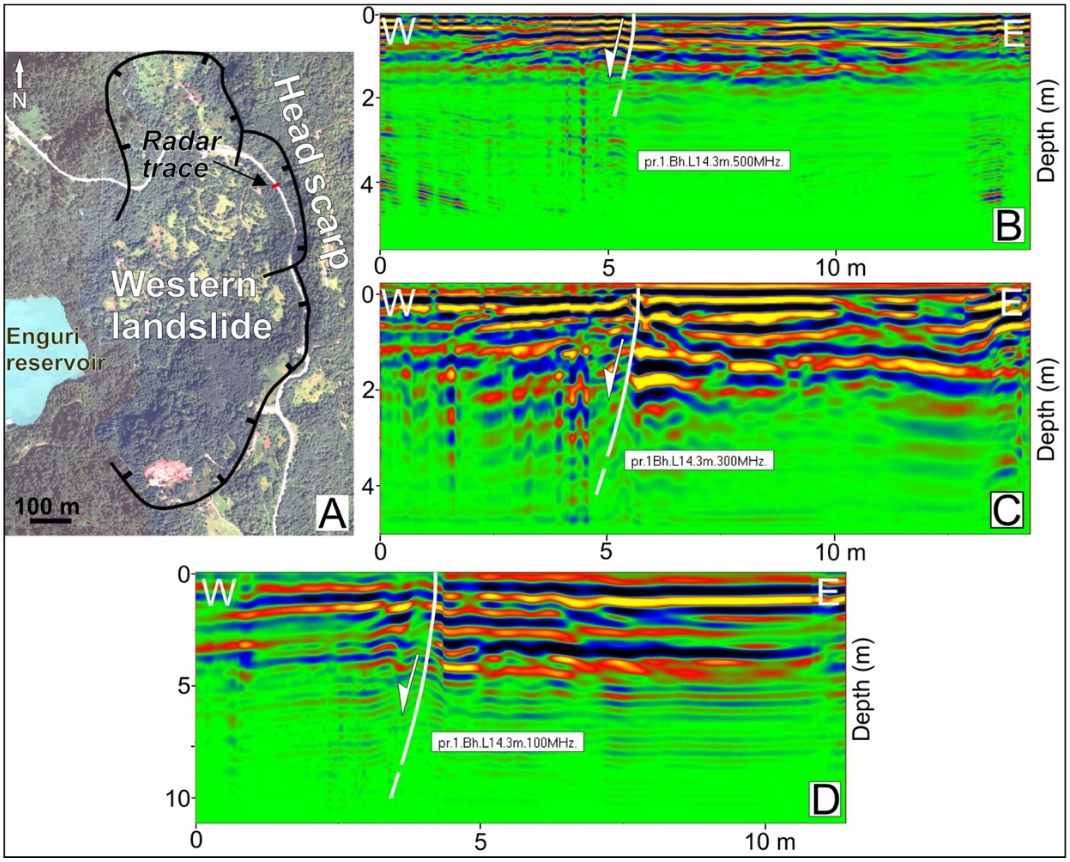

Figure 11: A. Location of the Ground Penetrating Radar (GPR) survey carried out in the western landslide across one of the active upper slip plane affecting the main road. The black line shows the uppermost head scarp of the landslide. B. GPR sections surveyed with an antenna at: B. 500 MHz, C. 300 MHz, and D. 100 MHz. The white lines represent the same slip plane.

3.5 Numerical modeling

To assess the stability of the slope, the depth of the possible slip surfaces, the contribution of the water table and its variation, comprising different lake levels, and gauge the impact of possible seismic shaking, we developed a series of numerical models of the western landslide. For the analyses, we used the program Slide of Rocscience 7.024, using the approaches of Janbu and Morgenstern-Price. For the seismic stability evaluation, we used the pseudostatic and Newmark modelling.

The slope stability analyses have been carried out based on the geological/geotechnical model that takes into account data coming from our field surveys, geotechnical tests and logs drilled during the Soviet era (1966) and by CGS (2015). The logs of 1966 are located in the lower slope, between 343 and 546 m a.s.l., in part in correspondence of the area now under the lake level; the more recent logs are located between 566 and 727 m a.s.l. (Fig. 7B). The reconstruction of the stratigraphy of

Nat. Hazards Earth Syst. Sci. Discuss., https://doi.org/10.5194/nhess-2018-186
Manuscript under review for journal Nat. Hazards Earth Syst. Sci.
Discussion started: 27 August 2018

Natural Hazards and Earth System Sciences
Open Access
Discussions

the landslide zone has been done by merging our field surveys with data coming from the logs n. 3291 (done in 1966), located at 403.62 m a.s.l., n. 3297 (1966) at 418.87 m a.s.l., n. 3261 (1966) at 435.62 m a.s.l., and n. BH1, BH3, BH4, BH5 and BH6 (done in 2015) located at 570-693.7 m a.s.l., and surveys made by Soviet researchers previous to the dam construction.

The present outcropping substrate is made of Jurassic volcano-sedimentary rocks, with interlayering of tuff deposits and sandstones, mostly dipping south (Fig. 7). The same rocks and bedding attitude was surveyed at the foot of the slope before the dam construction. These rocks are locally covered by Quaternary landslide and slope debris deposits. Based on their geotechnical characteristics, the succession has been divided into two geotechnical members: the deepest unit (in brown in Fig. 12) is given by the more intact tuffs and sandstones located below the surface located at a depth between 30 and 80 m. Above this surface, we considered a second geotechnical unit (in green in Fig. 12) made of clay, gypsum, debris and old landslide deposits. Debris contains dominant sandstones and tuff fragmented rocks, with a loam matrix, more rarely a clay matrix, rich in carbonatic and gypsum fragments. Locally, carbonatic fragments dominate. The thickness of this unit is from a few meters to a maximum of 80 m. These two units are covered by late Quaternary deposits that comprise colluvium, eluvium, and shallow debris, with a thickness from 1 to 5 m. These latter, shallow deposits have been incorporated in the geotechnical unit 2 (green unit), due to their low thickness and spatial variability. The geomechanical/geotechnical parameters obtained for the involved materials are presented in Table 1. Considering the high variability of deposits and thus of material properties, we performed a back analysis of the landslide to determine the appropriate material properties.

Figure 5A locates the piezometric wells that have been used to locate the depth of the water table. Our survey of piezometers showed the presence of water that during May 2017 reached the topographic surface (Table 2). In one well (BH9), the water table showed a temporary artesian behavior. The variation of the Enguri reservoir water level was established based on the information received from the Enguri Dam Company, which indicated the range 430-510 m a.s.l. Taking into account the low hydraulic conductivity of part of the deposits composing the studied slope, the large variations of lake level, and the intense rains that characterize this region, we focused on slope stability analyses that consider the stage of saturation of the involved deposits and did not carry out a transient slope stability analysis. The final material properties used for the modeling were derived based on back analysis and field observations and are presented in bold in Table 1. In particular, the used values of cohesion take into consideration the widespread presence of clastic debris deposits, locally reach in silty clays.

In the first static model, the reservoir water level is taken fixed at the maximum level (510 m) (Fig. 12A). The table water level inside the landslide body is assumed as complete saturation as indicated by piezometers during the rainy season. The model indicates that upper parts of the slope are unstable along curvilinear slip surfaces (orange lines) that correspond to Factor of Safety (FS) < 1. Most slip surfaces are shallow (10-30 m) and involve limited parts of the onshore slope.

In the second static model, the reservoir water level has been considered at minimum (430 m a.s.l.), resulting in more diffuse instability of the slope including the part normally below the lake. The relative slip surfaces (orange in Fig. 12B) correspond to FS < 1, and are mostly deeper (30-80 m) than in the previous case.

The pseudostatic numerical model was developed using a Peak Ground Acceleration (PGA) = 0.46 g obtained from the seismograph record (Fig. 13). We have chosen this record from the European strong motion database according to the Enguri

Nat. Hazards Earth Syst. Sci. Discuss., https://doi.org/10.5194/nhess-2018-186
Manuscript under review for journal Nat. Hazards Earth Syst. Sci.
Discussion started: 27 August 2018

Natural Hazards and Earth System Sciences
Discussions

local seismic conditions that take into account the typical earthquake fault mechanism solution and depth in the area, together with results obtained from deaggregation analysis of the hazard. Particularly, deaggregation has been used to select the earthquake of reference, which contributes most to the hazard. Probabilistic seismic-hazard deaggregation involves the determination of earthquake variables, such as magnitude and distance, defining seismic events that contribute to a selected seismic-hazard level (PGA or SA) (McGuire, 1995; Bazzurro and Cornell, 1999). The deaggregation results show that scenario calculations for obtained PGA value for a probability of exceedance of 10%, 5%, 2%, and 1% in 50 years should be made for a Mw = 6.9 earthquake at 18 km of distance from the landslide. The PGA was multiplied with a reference acceleration of 0. (Kavazanjian et al., 1997) to obtain seismic load coefficient = 0.07 (k_h = PGA x 0.17).

Table 1. Geo-mechanical properties of the deposits.

Rock/deposit	**Friction angle (ϕ')**	**Cohesion (c')**	**Specific weight (γ)**	**Data source**
Clay, measurements in borehole	10-18°	20-47 kPa	19.4-20.1 kN/m^3	(*)
Clay, collected at depth 16-17 m (SH2) and 51-51.2 m (SH4)	16-18°	44-47 kPa	19.2-19.5 kN/m^3	(*)
Weathered bedrock (heavy fractured rock with loam-clay filling)	32°	50 kPa	22 kN/m^3	(x)
Coarse clastic deposit	35-45°	0 kPa	22-23 kN/m^3	(x)
Intact bedrock	35°	200 kPa	25 kN/m^3	(x)
Shallow deposits	**16°**	**0.01-10 kPa**	**19.65 kN/m^3**	(+)
Bedrock	**32°**	**200 kPa**	**23.5 kN/m^3**	(+)

(*) Geotechnical Laboratory Tbilisi, (x) field observations and Hoek and Bray, 1981, (+) back analysis and field observations.

Table 2. Location of measured piezometers and water table depth.

Site	**Easting (dd.ddd)**	**Northing (dd.ddd)**	**Elevation (m asl)**	**Installed (MM/YY)**	**Installed depth (m bgs)**	**Measured depth to water (m bgs)**	**Measured depth to bottom (m bgs)**
BH1	42,049950	42,781550	566,6	07/15	45	7,4	35
BH2	42,050650	42,782500	568,2	07/15	50	1,5	36
BH3	42,049850	42,784583	587	07/15	32	1,3	16
BH4	42,050583	42,784417	652,8	07/15	65	1,3	16
BH5	42,052633	42,787150	679,7	07/15	50	0,0	42
BH5	42,052633	42,787150	679,7	07/15	50	0,5	42
BH6	42,053017	42,779717	725,9	07/15	50	12,0	18
BH7	42,055433	42,781700	721,3	07/15	50	5,8	49

Nat. Hazards Earth Syst. Sci. Discuss., https://doi.org/10.5194/nhess-2018-186
Manuscript under review for journal Nat. Hazards Earth Syst. Sci.
Discussion started: 27 August 2018

Natural Hazards and Earth System Sciences
Open Access
EGU
Discussions

BH8	42,055883	42,786517	704	07/15	55	4,8	23
BH9	42,051800	42,788767	702,6	07/15	51	-0,2	37
BH10	42,051800	42,790167	727,9	07/15	50	Destroyed	Destroyed

Table 3. Calculated values of PSH.

Vs30	**PSH10%**	**PSH5%**	**PSH2%**	**PSH1%**	**DH_0.5**
497	0.45	0.56	0.75	0.91	0.65
548	0.44	0.56	0.74	0.9	0.65
576	0.43	0.56	0.74	0.88	0.65
760	0.4	0.51	0.68	0.82	0.6

More in detail, the PGA value used in the present study has been appositely determined for the Enguri site, following these steps: we produced models of seismic source zones and their parameterization (estimate recurrence law, maximum magnitude, distribution of earthquakes depth, and nature of movement), using the catalogue of earthquakes that was created for Caucasus and Middle East Region by Zare at al. (2014, 2017) and seismic sources from Danciu et al. (2017). Then we developed appropriate ground motion prediction equation models and seismic hazard curves for spectral amplitudes at each period following the work of Danciu et al. (2016). Site characterisation was carried out based on ambient seismic noise registration "as single measurement" for HVSR (Horizontal to Vertical Spectral Ratio) application and active seismic velocity profiles by using Multichannel Analysis of Surface Waves (MASW). In total, we recorded up to ten ambient seismic noise measurements for the sites where we have also borehole data and performed six active seismic velocity profiles. Altogether site investigation was done for 16 points and Vs30 were estimated. Then, a digital elevation model (DEM) was prepared using topographic maps at a 1:2500 scale. The DEM was converted to a slope map and correlation between slope and Vs30 was adopted for the whole area of the landslide. Finally, Probabilistic Seismic Hazard (PSH) values were calculated for each point taking into account the site characteristics, for a probability of exceedance of 10%, 5%, 2%, and 1% in 50 years (Table 3).

The pseudostatic analysis is presented in (Fig. 14A) with the orange and red slip surfaces corresponding to FS < 1. Comparing the static (Fig. 12A) and pseudostatic analysis (Fig. 14A), it is evident that the susceptible slip surfaces are not just restricted to the upper part of the slope but extends all along the Quaternary deposits due to seismic shaking, and are deeper reaching the interface with the substratum. The full dynamic modeling of the slope to estimate the displacements expected from seismic shaking along the slope was done using the Newmark approach. The tolerable displacement is about 1 m (Kavazanjian et al., 1997) and any displacement > 1 m could lead to failure. It is evident from Newmark analysis (Fig. 14B - red slip circles represent failure surfaces that would experience displacements > 1 m) that the whole slope, down to the presently submerged slope toe and even parts of the bedrock, could experience displacements > 1 m. The estimated

Nat. Hazards Earth Syst. Sci. Discuss., https://doi.org/10.5194/nhess-2018-186
Manuscript under review for journal Nat. Hazards Earth Syst. Sci.
Discussion started: 27 August 2018

Natural Hazards and Earth System Sciences
Open Access
Discussions

displacements indicate that the slope is highly susceptible to seismic triggering and could lead to failure of the slope into the reservoir in the event of seismic activity compatible or greater than the PGA here calculated.

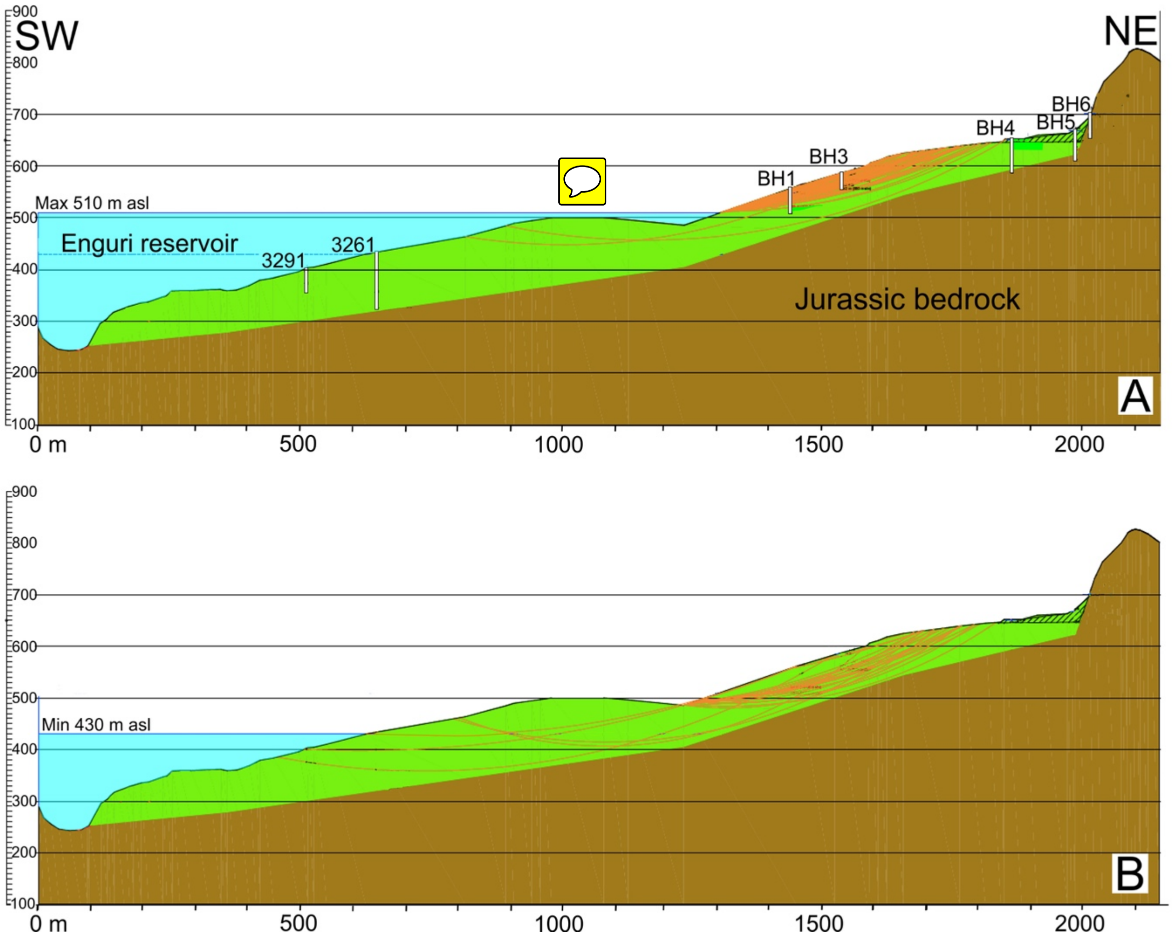

Figure 12: Sections of the static numerical modeling developed to analyze the effect of variation of the water level in the main landslide body. A. Instability developed with maximum level of the reservoir water level (orange lines = slip surfaces with FS < 1). B. Analysis of the effect of variation of the reservoir water level down to the minimum level; note new slip surface (with FS < 1) formation at lower elevations.

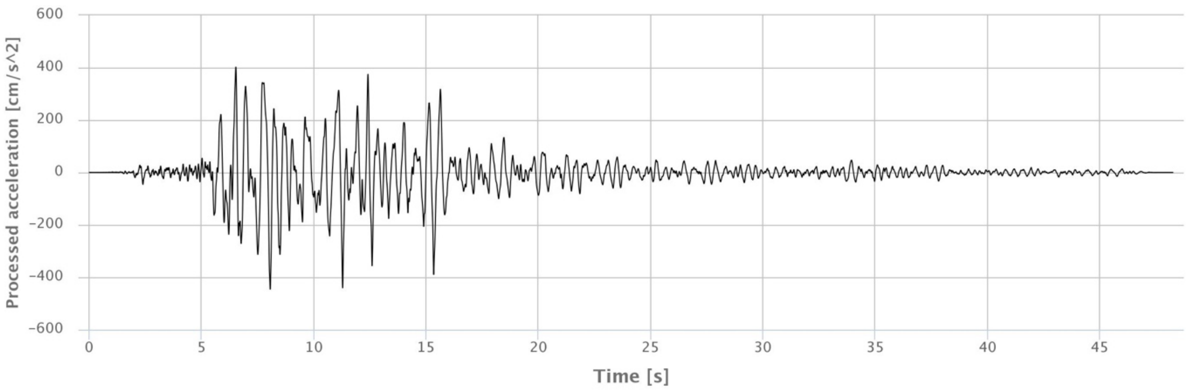

Figure 13: Seismic acceleration record used for the pseudostatic and Newmark slope stability analysis.

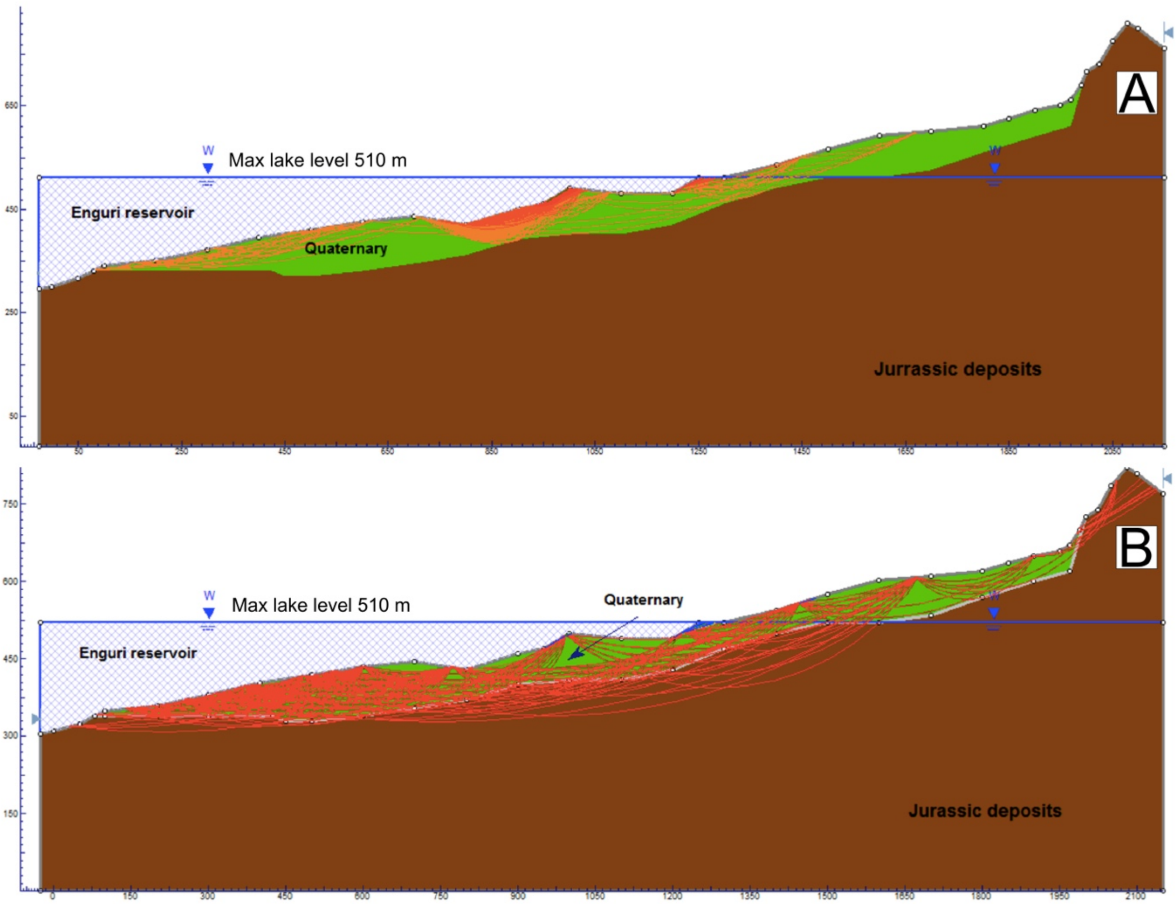

Figure 14: Results from seismic slope stability analysis. A. Pseudostatic numerical model showing the development of several potential slip surfaces (orange and red lines) with FS < 1. B. Dynamic modelling, by a Newmark approach,

Nat. Hazards Earth Syst. Sci. Discuss., https://doi.org/10.5194/nhess-2018-186
Manuscript under review for journal Nat. Hazards Earth Syst. Sci.
Discussion started: 27 August 2018

Natural Hazards and Earth System Sciences
Discussions

showing the development of several large slip surfaces (red lines) that would experience more than 1 m of displacement. Since 1 m is considered critical displacement that would yield to failure, these slip surfaces indicate very unstable conditions along the slope in case of an earthquake producing the calculated local seismic shaking.

3.6 Monitoring active deformation

Due to the evidence of active slope deformation, we installed two digital extensiometers (Wire Linear Potentiometric Transducer, SF500) that record in continuous the deformation across the upper scarp of the western landslide. One extensiometer was installed on 1 November 2016, and the other one a few months later. In Figure 15 we show the data collected at the older instrument (location at Trench 2, Fig. 6A), together with data regarding lake level variation, amount of rain, and internal and external (wire) temperatures, from 1 November 2016 to 15 may 2018. The total amount of deformation here is 67 mm in 18.5 months, which gives an average extension rate of 4.3 cm/y. Deformation largely increased from 16 May 2017 to 8 August 2017 with a total extension of 52 mm that corresponds to a rate of 0.61 mm/day (as a comparison, the average extension rate is 0.13 mm/day for the whole period of measurement). This interval of extension rate increase follows the almost complete drawdown of the lake (21 February 2017) and the successive period of lake level infilling, although a delay of about one month can be recognized. Another interval of rate increase, although much smoother than the previous one, is recognizable after 6 March 2018, in concomitance with another increase in lake level. During periods of lake level lowering, the extension here tends to decrease to minimum values. The amount of rain and temperature variations do not seem to affect the extension values.

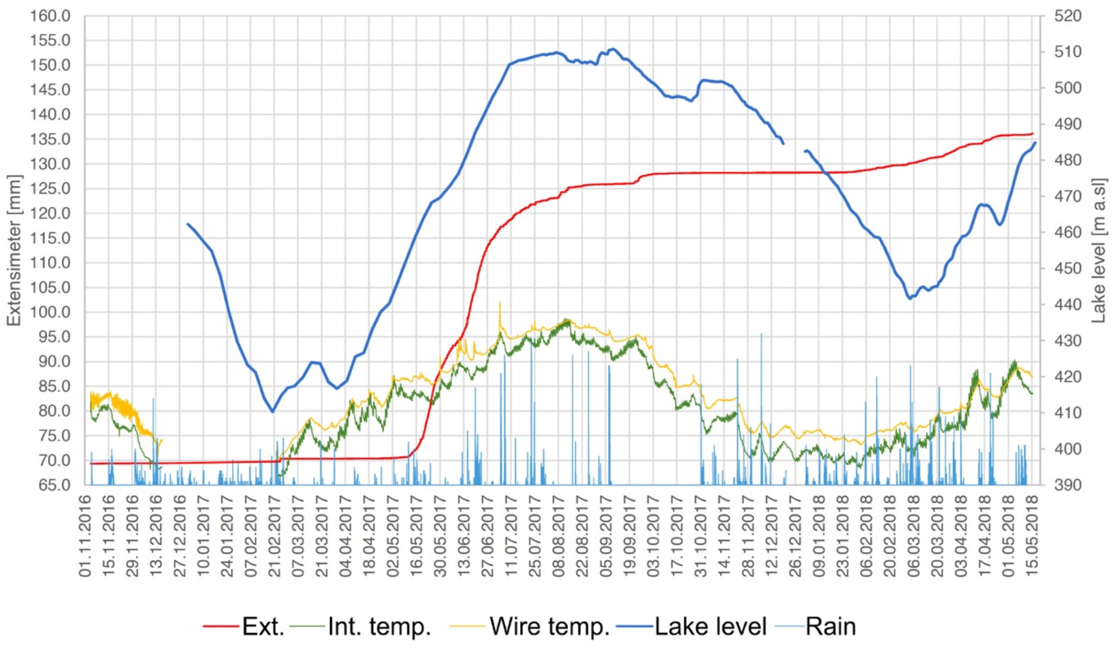

Figure 15: Data acquired at one of the two digital extensiometers located at the upper scarp of the western landslide (location Trench 2, Figure 6A). Blue line = lake level, Red line = extension, Yellow line = external (wire) temperature, Green line = internal temperature, Blue segments = rain amount.

4 Discussion

4.1 Evidence of active landsliding

In the study area, we found several evidences of active slope deformation that affect the same mountain ridge on both the western and eastern flanks. Although part of the western landslide was already locally known as Khoko, this is the first time that its characteristics are reported in the scientific literature, whereas the eastern landslide has never been recognized before. For example, in the Geoportal of Natural Hazards and Risks in Georgia (http://drm.cenn.org), in the section dedicated to landslide hazard, the map reports a medium landslide hazard at all the slopes located east of the Enguri reservoir, without distinction in correspondence of the large, active structures presented in our paper.

Regarding the western landslide, the data here presented allowed to define its real total dimension, suggesting that the unstable slope area is larger than the previously known Khoko landslide. We recognized the presence of a main head scarp that runs upward respect to the Jvari-Khaishi-Mestia road (i.e. east of the road, Fig. 5A) in the northern-central part, then crosses the road and runs west of it. This scarp is made of three main segments with the concave side (in plan view) facing west. The segments are interconnected and thus the total head scarp is continuous suggesting that the process of slope instability has already led to link together what originally might have been a series of discrete landslides. Historical and present-day activity along this landslide is manifested by the presence of fissures and slip planes at the foot of the head scarp, subsidiary scarps in the slope, and systematic tilted trees all along the slope. Where the Jvari-Khaishi-Mestia road crosses the active structures, it requires continuous maintenance in order to fill the opening fractures and smooth the scarps created along the slip planes.

The eastern landslide shows a main head scarp that runs upward respect to the Jvari-Khaishi-Mestia road (i.e. west of the road, Fig. 9). It is made of a single structure with the concave side (in plan view) facing east. The height of the scarp is in the order of 3-20 m, although it is difficult to quantify it precisely due to the local presence of dense vegetation. Historical and present-day activity along this landslide is manifested by the presence of fissures along the head scarp, some of which are located in the forest and some cross the Jvari-Khaishi-Mestia road that also here requires continuous maintenance. Moreover, an old concrete wall shows 1.9 m of left-lateral strike-slip offset compatible with landslide movements along the lateral slip plane.

4.2 An old history of slope deformation

We found evidence that the studied western slope has a long history of landsliding. The geological map surveyed during Soviet times, before the infilling of the water reservoir, shows the presence of prehistoric landslide deposits, with a thickness up to 35-40 m, at the lower part of the slope, now submerged (see Fig. 3 and section in Fig. 7B). Moreover, at the foot of the present onshore slope, there are gypsum deposits extremely deformed, which should result from a long history of movements. There are also several evidences suggesting that both the western and eastern landslides have started their movements at least several tens of years ago. The western landslide was already moving during the construction of the pavement of the old Jvari-Khaishi-Mestia road. This road was improved during the construction of the Enguri dam, at the Soviet era, by putting a very thick concrete flooring, as showed in Trench 1 that we opened across one of the active slip planes located at the foot of the head scarp (Fig. 6C). The thickness of 0.5 m of this concrete layer and its presence suggest that it was required possibly due to the recognition at that times of active deformation along this road segment. In fact, during the Soviet era, the general thickness of concrete roads was much lesser. Moreover, the concrete pavement is lowered of 1.3 m respect to the present road level, confirming an ongoing process of subsidence here. Then it was followed by the construction of a further road, found 20 cm below the present road level in Trench 1 and 2, which also confirms continuous downsagging of the area. Here, the present-day road surface suffers of continuous offsetting with consequent necessity to accumulate further tens of cm of asphalt to maintain the road level.

Also the eastern landslide has evidence of an old history; first of all, at the foot of the head scarp there is a lake, measuring 43 x 17 m, with the long axis parallel to the local scarp strike (Fig. 9). The lake is associated with clay deposits that require times for their formation. Where the head scarp of the landslide comes closer with the head scarp of the other western landslide, there is the series of long and wide fissures in the densely-vegetated forest (e.g. Fig. 5D, and Fig. 9). These fissures host several tree trunks whose dimension suggests they are at least some tens of years old. Moreover, several hand-made structures show incremental offset with age (the concrete wall of the 70' ys, the water channel, the white strips of the asphalt, etc.) confirming the gradual continuous movements of this landslide.

4.3 Kinematics

The height of the head scarp of the western landslide is in the order of 20-70 m, showing that the landslide suffered important vertical slip in the head zone. The presence of a wide sub-horizontal to gentle slope at the scarp foot, which has been exploited for the construction of the Jvari-Khaishi-Mestia road, associated with the presence of the head scarp, suggest the development of rotational movements of the upper slope. Ongoing development of vertical scarps in the asphalt of the road, and the presence of gentle scarps in the middle slope, indicate that rotation movements are still present in different zones of the landslide area. Dip-slip movements along subvertical planes are confirmed by the GPR survey. The orientation of the active fissures and slip planes surveyed on the road, which are parallel to subparallel to the main head scarp, and the presence of dip-slips along the vertical scarps, indicate a general movement of this western landslide towards the west. In detail, the movement is more complex since the northern part shows motions towards SSW, the central part toward W, and the southern part toward NW. These vectors, together with the general shape of the landslide in plan view, suggest that there is a concentric movement of the landslide body towards the toe zone, where bulging and decrease of motion are expected. Anyway, since the tow zone is under the Enguri lake, it is impossible to verify what occurs in the lowermost part of the landslide.

In regard to the eastern landslide, in the field there is clear indication of several meters of vertical slip along the head scarp, at the foot of which there is a flat area that contains the small lake. A portion of this sub-horizontal area has been exploited also here to host the Jvari-Khaishi-Mestia road. These data indicate the presence of rotational movements of the upper slope. The northern lateral boundary of the landslide is characterized by a prolongation of the main head scarp that crosses the road. In this point, there is the 70'-ys-old concrete wall that shows tilting northward compatible with a component of downthrown of the southern block. This dip-slip component is confirmed by the GPR surveys, as can be appreciated in the sections of Fig. 10. The same wall also shows the 1.9 left-lateral strike-slip offset that is compatible with the general eastward motion of the landslide body. The northern boundary of the landslide is thus characterized by transtensional movements that also comply with rotational deformation of the upper part of the unstable slope. Along the southern part of the GPR section of Fig. 10, strata are tilted southward, although the close southward dip of the slip plane visible in the section is compatible with an opposite versus of tilting. We suggest that this strata tilting in reality is connected with the southern lateral boundary of the landslide that is located more southward respect to this GPR section (see Fig. 10A). This boundary is given by a slip plane that here dips to the NE and, as a consequence, should produce tilting of strata towards SW.

4.4 Slip rates

For the western landslide, Trench 1 allows to estimate a long-term (57 ys) slip rate of the vertical component of motion in the order of 2.3 cm/y, based on the age of the oldest buried road made about AD 1960. Our repeated observations on the development of fissures and vertical scarps onto the asphalt of the modern road surface, conducted in the years 2015-2017, indicate slip-rates between < 1 cm/y up to 9 cm/y, depending on the location of the examined structure. We remind that these features are usually destroyed during restoring of the asphalt pavement. The data of the installed extensiometer indicate an extension rate of 4.3 cm/y in the last 1.5 years. In general, it seems that the slip rate increases from south to north along the upper part of the landslide, although this observation requires detail measurements to be confirmed. For this reason, we installed a network of 18 bench marks distributed all along the upper part of the landslide. GPS measurements started in the late 2016 and will be published in a future paper.

At the eastern landslide, the 190 cm offset of the concrete wall (November 2015) and its age of AD 1974, result in a slip rate of 4.6 cm/y for the long-term (41 ys) motion towards east. The same wall's offset has been re-measured in May 2017 showing a total dislocation of 195 cm, and a resulting short-term slip-rate of 3.75 cm/y. The water channel offset was measured between November 2015 and May 2017 giving a short-term slip rate of 1.5 cm/y. The offsets amount and age of the white strips on the road, give estimation of 4 cm/y for the short-term slip rate (2 ys). We remind that also here the road deformation features are destroyed during periodic restoring of the asphalt pavement.

4.5 Possible origin of slope deformation

As regards the dimension and type of the western landslide, for which more data are available, it is necessary to stress that this slope is characterised by the presence of a thick shallow succession of debris and clay-gypsum deposits in the order of at least 30-80 m. This indicates the presence of a thick sequence of deposits that have poor mechanical properties and that are widespread all over the investigated slope. In fact, the numerical models, both static and dynamics, indicate the possible development of several slip planes (characterised by FS < 1). In particular, the dynamic modelling shows slip surfaces with FS < 1 that reach depths in the order of 80–100 m. In the field, there are clear evidence of rotational deformation in the upper part of the unstable slope, accompanied by dip-slip along the planes perpendicular to the general downhill motion. Finally, our preliminary GPS measurements of bench marks in the upper slope indicate a clear consistent pattern of slope motion and homogenous GPS velocity. All these data do not fit with the interpretation of slope deformation linked to scattered, discrete surficial small landslides, but are instead consistent with a slope affected by a unique landslide. Based on numerical simulations, the depth of the possible slip surfaces that might develop especially under earthquake solicitation, indicates a probable DSGSD.

The similar position and features of the western and eastern landslides cannot be a mere series of coincidences, and we cannot exclude that they have a common origin. The toe of the two unstable slopes are located at 400-300 m a.s.l., which correspond to the level of erosion of the present river located at the foot of the eastern landslide, and to the original river level at the base of the western landslide, now hidden below the Enguri water reservoir. The two river valleys have a *V*-geometry in section view and interest areas mostly at altitudes lower than 1900 m a.s.l., that represents the lower threshold of former glaciers of the Late Glacial Maximum phase (Late Pleistocene) defining the lower boundary of the nival zone (Gobejishvili et al., 2011). This means that the two river valleys might have started to form before the LGM, but they fully developed down to the present depth in consequence of the post-LGM water runoff. Both valleys reach the common flood plain of the Rioni Basin at the same altitude. All these features suggest that the two river valleys developed at the same time, contributing to create the topographic gradient at the two sides of the mountain ridge. Based on all this information, we suggest that the triggering factor in the development of the two landslides might have been the increase above a threshold value of the slope dip and of the topographic altitude difference created by river erosion.

The formation of the two deep river valleys and the consequent development of the mountain ridge that gave rise to the two landslides, may also be linked with the mountain uplift of the region. An increase in Plio-Pleistocene exhumation rates in northwest Georgia is supported by thermochronometric studies (Vincent et al., 2011) that show the southern flank of the western Greater Caucasus range has undergone rapid exhumation of ~ 1 km/Ma since the Pliocene onwards. In particular, the geological structural setting of the study area is characterized by the presence of thickening of the shallow crustal succession caused by thin-skin tectonics (Fig. 16). The structural section portrayed in this figure has been obtained by integrating our field surveys with geophysical and geological data from Banks et al. (1997). The section shows the presence of a main basal thrust dipping north. The basal thrust has a ramp-flat geometry that produced a frontal asymmetric ramp anticline. This structure clearly produces local enhanced uplift in correspondence of the ramp anticline, exactly where our study area is located (see box in Figure 16). Moreover, other small reverse faults are located in the area, contributing to further uplift. Under this structural architecture, and taking into account the seismic activity of western Caucasus (Tsereteli et al., 2016), an earthquake with the consequent ground acceleration cannot be ruled out as possible triggering of one of the two landslides or of both.

Nat. Hazards Earth Syst. Sci. Discuss., https://doi.org/10.5194/nhess-2018-186
Manuscript under review for journal Nat. Hazards Earth Syst. Sci.
Discussion started: 27 August 2018

Landslides aligned along active faults and triggered by seismic activity have been observed frequently elsewhere (e.g. Tibaldi et al., 1995, 2015). Anyway, the available seismic catalogue goes back in the area up to the Tsaishi earthquake of 1614 AD (Tibaldi et al., 2017b), and thus does not allow to establish a possible direct relationship, also in view of the fact that the exact age of inception of these landslides is unknown.

A gross estimation of the possible age of the studied landslides can be done if we assume a constant deformation rate; for the western landslide, with the average height of the head scarp (45 m) and average slip rate (3 cm/y), we obtain a rough age of the landslide in the order of 1500 ys. At the eastern landslide, the average height of the head scarp (30 m) and average slip rate (3.5 cm/y), give a gross age estimation in the order of 900 ys.

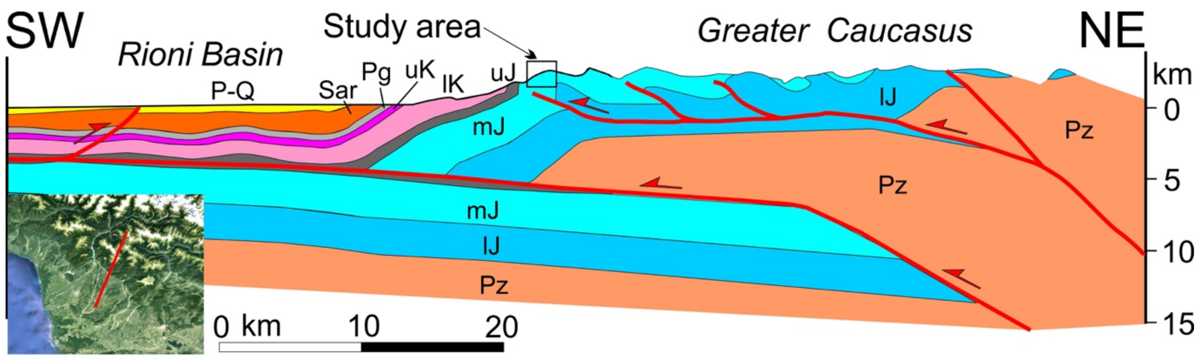

Figure 16: Structural section passing throw the study area (box), obtained by integrating our field surveys with geophysical and geological data from Banks et al. (1997). Note the presence of a main basal thrust dipping north, which shows a ramp-flat geometry that produced a frontal asymmetric ramp anticline.

4.6 Hydrogeological hazard

Although this is a preliminary description of the evidence and characteristics of the landslides located nearby the Enguri dam, the data here presented are enough to pinpoint a series of relevant results on the hydrogeological hazard of the area. First of all, the western landslide faces directly the Enguri reservoir, with the toe zone of the unstable slope located below the water level, as resulting from the pseudostatic and dynamic numerical analyses that are justified by the fact that the studied area is located in an active tectonic region where earthquakes with Ms up to 7.0 have been recorded (Varazanashvili et al., 2011). This slope moves continuously in a sort of creeping, as already observed elsewhere at DSGSDs (Varnes et al., 1989, 1990, 2000). Anyway, it has been also observed that movements at DSGSDs can be intermittent (Beget, 1985): they can slow down or stop, and then suddenly unrest with rapid downward displacement also in the order of meters, without a complete failure (Tibaldi et al., 2004; Tibaldi and Pasquaré, 2008; Pasquaré Mariotto and Tibaldi, 2016). Anyway, the occurrence of a sudden downhill displacement of the western landslide, for example during seismic shaking as indicated by the Newmark analysis, can involve a huge rock volume, in the order of $48 \pm 12*10^6$ m^3. This might have effect on the water body, and this hypothesis is worth further studies on the topic.

Nat. Hazards Earth Syst. Sci. Discuss., https://doi.org/10.5194/nhess-2018-186
Manuscript under review for journal Nat. Hazards Earth Syst. Sci.
Discussion started: 27 August 2018

Natural Hazards and Earth System Sciences
Discussions

Our preliminary static numerical modelling suggests that slope movements can occur both when the lake is at the highest level and when it is lowered. This result does not necessarily suggest a possible catastrophic failure of the slope in static conditions, but is instead coherent with the field evidence of continuous deformation along the slope. We interpret this as a consequence of the characteristics of the deposits along the slope. Slip surfaces can activate especially in the part of the slope above the lake level, because here deposits rich in clays, and very altered tuffs, dominate. When the water table lowers from 510 m to 430 m, although a rapid drawdown condition is created, the shallow deposits of the upper slope remain saturated due to their low hydraulic conductivity. Moreover, increase of movements can occur during phases of saturation of the on-shore landslide body that may take place particularly during the rainy season. At the lowest lake level, slip surfaces can activate in the lower part of the slope due to debuttressing of the slope toe, although the dominance here of deposits with a relatively high hydraulic conductivity.

The two studied landslides also pose a threat to other infrastructures like the Jvari-Khaishi-Mestia road, which in fact requires continuous maintenance to avoid the gradual formation of dangerous, tens of decimetres high steps in the asphalt. We highlight also the presence of an inhabited house resting in the middle of the western landslide, and another house recently built close to the northern boundary slip zone of the eastern landslide.

In order to contribute to a better assessment of the hydrogeological hazard of the area, we installed two digital extensiometers in correspondence of the active head structures of the western landslide, together with the already mentioned bench marks for GPS measurements. This monitoring effort will help to individuate possible alert situations and to better constrain the behaviour of this unstable slope.

4.7 Comparison with other landslides

Here we focus on the western landslide, its relations with the artificial lake, and similar settings reported by literature. As shown by the Quaternary geological deposits and by the presence of the high head scarp, the studied area was already interested by the emplacement of landslide deposits in prehistoric times. The already destabilized slope was thus interested by the formation of the Enguri reservoir and its level variations. The creation of artificial lakes can have different effects: on one side, it triggers possible seepage process resulting in an increase in pore water pressure within the slope deposits, thus reducing their shear strength. On the other side, the presence of the lake water body induces a stabilizing load at the toe of the submerged part of the slope (Paronuzzi et al., 2013). In transient conditions, the rate of lake filling or drawdown, combined with the permeability of the bank-forming materials, produce different effects of reservoir level changes. Several landslides, in fact, have been triggered by filling–drawdown operations (Schuster, 1979; Kenney, 1992; Zhu et al., 2011), as well as pre-existing, ancient landslides have been reactivated during water reservoir formation (e.g. Kaczmarek et al., 2015).

In the case of low permeability of slope materials, rapid drawdown of the lake level can produce a decrease in the factor of safety, possibly leading to slope failure (Kenney, 1992). A rapid decrease in lake level, in fact, results in a short-term increase in hydraulic gradient in adjacent slopes (Jones et al., 1961; Schuster and Wieczorek, 2002; Deying et al., 2010; Pinyol et al., 2012). For example, in Japan about 60% of reservoir landslides occurred during sudden decrease of the water level

(Nakamura, 1990). At a DSGSD located above the Gepatsch dam reservoir (Austrian Alps), slope deformation rates correlate with reservoir levels and drawdown conditions (Zangerl et al., 2010). In the case, instead, of high permeability of bank-forming materials, the reservoir level increase can produce a decrease in the factor of safety. For example, at the Vajont (Italy) catastrophic landslide, detailed numerical analyses by Paronuzzi et al. (2013) show the predominant role played by reservoir levels in determining slope instability, respect to the rain-induced water table in the upper slope. In particular, the initial large slope deformation took place in concomitance with the lake level rise. Consistent with this trend, the final collapse of 9 October 1963 coincided with the maximum reservoir level reached. Paronuzzi et al. (2013) also show that the decisive geological factor contributing to the Vajont collapse was the presence of an already existing landslide: the prehistoric rockslide was characterized by materials with high permeability and a thick shear zone at the base, including montmorillonitic clay lenses. The combination of poor mechanical properties of clay beds with the high permeability of the angular limestone gravel, determined a rapid reservoir-induced inflow that reduced strength and factor of safety. A further example is given by the Byford Creek slide, located above the Clyde Dam reservoir (New Zealand). Here, long-term creep movements show a clear reaction to lake filling, with a first large increase in the deformation rate and long-term slowing of movement (Macfarlane, 2009).

The landslide here studied, at distance of more than 40 years from the construction of the Enguri reservoir, still shows a high sensitivity to water infilling operations. The unstable slope behavior, during large water level variations, is similar to other landslides with bank-slope material characterized by high permeability. In particular, the deposits found in the logs of the lower part of the slope (below about 500 m a.s.l.), being characterized by the dominance of angular carbonatic clasts with interspersed clays, recall those present at other landslides where the factor of safety decreases with increase of lake level. With such characteristics of the involved materials, during reservoir increase the pore water pressure effect on the shear strength prevails over the stabilizing buttressing of the lake water body, inducing an acceleration in slope movements. This is testified by the acceleration in slope deformation following the Enguri reservoir infilling (Fig. 15).

5 Conclusions

We presented for the first time the evidence and characteristics of two large landslides located nearby the Enguri dam and water reservoir, in the southwestern part of the Caucasus (Republic of Georgia).

The landslides affect the two opposite slopes of a mountain ridge that runs parallel to the Enguri reservoir. The slope directly facing the reservoir shows active deformations that involve a subaerial area of 1.2 km^2. Field data, Ground Penetrating Radar surveys, information coming from wells, seismological data with calculation of the local Peak Ground Acceleration (PGA), and numerical modelling, indicate different depths of the possible sliding surfaces depending on various parameters. The worst scenario is given by the occurrence of a PGA compatible with the highest seismicity of the region, which can contribute to activate slip surfaces at depths corresponding to a volume of the unstable mass up to $48 \pm 12*10^6$ m^3.

The head scarp zones of both landslides interest the main Jvari-Khaishi-Mestia road with offsets of man-made features that indicate short-term (last 2 years) slip rates up to 9.3 cm/y and long-term (last 55 years) slip rates up to 4.6 cm/y.

Nat. Hazards Earth Syst. Sci. Discuss., https://doi.org/10.5194/nhess-2018-186
Manuscript under review for journal Nat. Hazards Earth Syst. Sci.
Discussion started: 27 August 2018

Natural Hazards and Earth System Sciences
Open Access
Discussions

The possible causes for the past inception of the two landslides can be multiple. First of all, we propose the increase above a threshold value of the slope dip and of the topographic altitude difference created by river erosion. The toe zones of both landslides, in fact, are located in correspondence of deeply entrenched rivers; the river's location at the foot of the western landslide is now below the Enguri water reservoir. The excavation of the two parallel river valleys, in turn, can be linked with the increase in Plio-Pleistocene exhumation rates of this mountain area of ~ 1 km/Ma. The study area, in particular, is located above an anticlinal fold linked with a ramp thrust fault. A tectonic seismic mechanism, with the consequent ground acceleration, cannot be ruled out as possible triggering of one of the two landslides or of both.

Extensiometer measurements across the head scarp of the western landslide, indicate a present-day variable deformation (average 4.3 cm/y). The deformation rate variations are poorly consistent with rain amount, whereas extensiometer data suggest that the landslide body is more sensitive to reservoir filling operation, in consequence of the geotechnical characteristics of the bank-slope materials. During large lake level decrease, the low hydraulic conductivity of the upper slope may contribute to increase movements in the onshore part of the slope. During large lake level increase, the higher permeability of the deposits of the lower slope, mostly constituted by ancient landslide deposits and slope debris, may facilitate acceleration in slope motion.

Competing interests

The authors declare that they have no conflict of interest.

Acknowledgments

This study has been conducted in the framework of the NATO project SfP G4934 "Georgia Hydropower Security", of the International Lithosphere Program - Task Force II, of the European Space Agency project n. 32309 "Active tectonics and seismic hazard of southwest Caucasus by remotely-sensed and seismological data" (Leader A. Tibaldi), and of project 216758 of the Shota Rustaveli National Science Foundation.

References

Adamia, Sh., Lordkipanidze, M. B., and Zakariadze, G. S.: Evolution of an active continental margins exemplified by the alpine history of the Caucasus, Tectonophysics, 40, 183-199, 1977.

Adamia, Sh., Alania, V., Chabukiani, A., Chichua, G., Enukidze, O., and Sadradze, N.: Evolution of the Late Cenozoic basins of Georgia (SW Caucasus): a review, In: Sedimentary basin tectonics from the Black Sea and Caucasus to the Arabian Platform (eds. M. Sosson, N. Kaymakçı, R. Stephenson, F. Bergerat), Geological Society, London, Special Publication, 340, 239-259, 2010.

Nat. Hazards Earth Syst. Sci. Discuss., https://doi.org/10.5194/nhess-2018-186
Manuscript under review for journal Nat. Hazards Earth Syst. Sci.
Discussion started: 27 August 2018

Adamia, Sh., Alania, V., Tsereteli, N., Varazanashvili, O., Sadradze, N., Lursmanashvili, N., and Gventsadze, A.: Post-Collisional Tectonics and Seismicity of Georgia. In: Tectonic Evolution and Seismicity of south-west Asia. Geological Society of America (GSA) Special Paper (in press), 2017.

Adamia, Sh., Zakariadze, G., Chkhotua, T., Chabukiani, A., Sadradze, N., Tsereteli, N., and Gventsadze, A.: Geology of the Caucasus: A Review, Turkish Journal of Earth Sciences, 20, 489–544, 2011.

Alania, V., Chabukiani, A., Chagelishvili, R., Enukidze, O., Gogrichiani, K., Razmadze, A., and Tsereteli, N.: Growth structures, piggyback basins and growth strata of Georgian part of Kura foreland fold and thrust belt: implication for Late Alpine kinematic evolution. In Tectonic Evolution of the Eastern Black Sea and Caucasus (eds M. Sosson, R. Stephenson & Sh. Adamia), Geological Society of London, Special Publications, 428, doi:10.1144/SP428.5, 2016.

Avagyan A., Sosson, M., Karakhanian, A., Philip, H., Rebai, S., Rolland, Y., Melkonyan, R., and Davtyan, V.: Recent tectonic stress evolution in the Lesser Caucasus and adjacent regions, In. Sosson, M., Kaymakci, N., Stephenson, R. A., Bergerat, F. & Starostenko, V. (eds), Sedimentary Basin Tectonics from the Black Sea and Caucasus to the Arabian Platform. Geological Society, London, Special Publications, 340, 393–408, DOI: 10.1144/SP340.17 0305-8719/10, 2010.

Avdeev, B., and Niemi N. A.: Rapid Pliocene exhumation of the central Greater Caucasus constrained by low-temperature thermochronometry, Tectonics, 30, TC2009, doi:10.1029/2010TC002808, 2011.

Banks, C., Robinson, A., and Williams, M.: Structure and regional tectonics of the Achara-Trialeti fold belt and the adjacent Rioni and Kartli foreland basins. Republic of Georgia, In Regional and Petroleum geology of the Black Sea and Surrounding Region (ed. A. G. Robinson), American Association of Petroleum Geologists Memoir no. 68, 331-336, 1997.

Barrier, E., and Vrielynck, B.: Palaeotectonic Map of the Middle East, Atlas of 14 Maps, Tectonosedimentary-palinspastic Maps from Late Norian to Pliocene, Commission for the Geological Map of the World, Paris, 2008.

Bazzurro, P., and Cornell, C. A.: Deaggregation of seismic hazard, Bull. Seism. Soc. Am., 89, 501–520, 1999.

Beck, A.C.: Gravity faulting as a mechanism of topographic adjustment, New Zealand Journal of Geology and Geophysics, 11, 191–199, 1968.

Beget, J.E.: Tephrochronology of antislope scarps on an alpine ridge near Glacier Peak, Washington, U.S.A. Arctic and Alpine Research, 17, 143-152, 1985.

CGS (Center Geodynamic Studies L.L.C.): Implementation of a complex engineering-geological survey of the left bank of the landslide in the reservoir area of arch dam LLC «Enguri HPP» and slope stability analysis, Technical report, Moscow, 2015.

Chigira, M., and Kiho, K.: Deep-seated rockslide avalanches preceded by mass rock creep of sedimentary rocks in Akaishi Mountains, central Japan, Engineering Geology, 38, 221-230, 1994.

Nat. Hazards Earth Syst. Sci. Discuss., https://doi.org/10.5194/nhess-2018-186
Manuscript under review for journal Nat. Hazards Earth Syst. Sci.
Discussion started: 27 August 2018

Danciu, L., Kale, O., and Akkar, S.: The 2014 earthquake model of the Middle East: ground motion model and uncertainties, Bull. Earthquake Engineering, 1-37, 2016.

Danciu, L., Şeşetyan, K., Demircioglu, M., Gülen, L., Zare, M., Basili, R., Elias, A., Adamia, S., Tsereteli, N., Yalçın, H., Asif Khan, M.U.M., Saya, M., Hessami, K., Rovida, A., Stucchi, M., Burg, J.-P., Karakhanian, A., Babayan, H., Avanesyan, M., Ammadli, T., Al-Qaryouti, M., Kalafat, D., Varazanashvili, O., and Erdik, M.: The 2014 earthquake model of the Middle East: seismogenic sources, Bulletin of Earthquake Engineering, 1-32, DOI: 10.1007/s10518-017-0096-8, 2017.

Deying, L., Kunlong, Y., and Chin, L.: Analysis of Baishuihe landslide influenced by the effects of reservoir water and rainfall, Environ. Earth Sci., 60, 677–687, doi:10.1007/s12665-009-0206-2, 2010.

Evans, S.G., and Couture, R.: The 1965 Hope Slide, British Columbia; catastrophic failure of a sagging rock slope, Abstracts with Programs-Geological Society of America, 16-26, 2002.

Forte, A., Cowgill, E., Bernardin, T., Kreylos, O., and Hamann, B.: Late Cenozoic deformation of Kura fold-thrust belt, southern Greater Caucasus, Geological Society of American Bulletin, 122, 465-86, 2010.

Gobejishvili, R., Lomidze, N., and Tielidze, L.: Late Pleistocene (Würmian) Glaciations of the Caucasus, In J. Ehlers, P.L. Gibbard and P.D. Hughes, editors: Developments in Quaternary Science, 15, 141-147, ISBN: 978-0-444-53447-7, 2011.

Gutiérrez-Santolalla, F., Acosta, E., Rıos, S., Guerrero, J., and Lucha, P.: Geomorphology and geochronology of sackung features (uphill-facing scarps) in the Central Spanish Pyrenees, Geomorphology, 69, 298-314, 2005.

Hoek, E., and Bray, J.W.: Rock Slope Engineering, Revised third edition, The Institution and Metallurgy of Mining, London, 1981.

Jones, F.O., Embody, D.R., and Peterson, W.L.: Landslides along the Columbia River Valley, Northeastern Washington, US Geological Survey Professional Paper, 367, 1961.

Kaczmarek, H., Tyszkowski, S., and Banach, M.: Landslide development at the shores of a dam reservoir (Włocławek, Poland), based on 40 years of research, Environmental Earth Sciences, 74(5), 4247-4259, 2015.

Kavazanjian, Jr, E., Matasovic, N., Hadj-Hamou, T., and Sabatini, P. J.: Geotechnical Engineering Circular No. 3: Design Guidance, Geotechnical Earthquake Engineering for Highways. Volume I-Design Principles (No. Report No: FHWA-SA-97-076), 1997.

Kenney, T.C.: Slope stability in artificial reservoirs: influence of reservoir level, selected cases, and possible solutions, In: Semenza, E., Melidoro, G. (Eds.), Proceedings of the meeting on the 1963 Vajont landslide, 17-19 September 1986, Ferrara, Cansiglio and Vajont. Grafica Ferrarese, Ferrara, Italy, 67-85, 1992.

Koçyiğit, A., Yılmaz, A., Adamia, S., and Kuloshvili, S.: Neotectonics of East Anatolia Plateau (Turkey) and Lesser Caucasus: Implication for transition from thrusting to strike-slip faulting, Geodinamica Acta, 14,177-195, 2001.

Macfarlane, D.F.: Observations and predictions of the behaviour of large, slow-moving landslides in schist, Clyde Dam reservoir, New Zealand, Engineering Geology, 109(1-2), 5-15, 2009.

Mahr, T.: Deep-reaching gravitational deformations of high mountain slopes, Bulletin of the International Association of Engineering Geology, 16, 121-127, 1977.

McCalpin, J.: Criteria for determining the seismic significance of sackungen and other scarplike landforms in mountainous regions. Techniques for Identifying Faults and Determining their Origins, U.S. Nuclear Regulatory Commission, Washington, 255–259, 1999.

McCalpin, J.P., and Irvine, J.R.: Sackungen at the Aspen Highlands ski area, Pitkin County, Colorado, Environmental and Engineering Geoscience, 1, 277-290, 1995.

McGuire, R. K.: Computations of Seismic Hazard, Annali di Geofisica, 36, 181-200, 1995.

Meijers, M.J., Smith, B., Kirscher, U., Mensink, M., Sosson, M., Rolland, Y., Grigoryan, A., Sahakyan, L., Avagyan, A., Langereis, C., and Müller, C.: A paleolatitude reconstruction of the South Armenian Block (Lesser Caucasus) for the Late Cretaceous: Constraints on the Tethyan realm, Tectonophysics 644, 197–219, 2015.

Mosar, J., Kangarli, T., Bochud, M., Glasmacher, U. A., Rast, A., Brunet, M., Sosson, M.: Cenozoic–Recent tectonics and uplift in the Greater Caucasus: a perspective from Azerbaijan, In: Sedimentary basin tectonics from the Black Sea and Caucasus to the Arabian Platform (eds. M. Sosson, N. Kaymakçı, R. Stephenson, F. Bergerat), Geological Society, London, Special Publication, 340, 261–279, 2010.

Nakamura, K.: On reservoir landslide, Bulletin on Soil and Water Conservation, (In Chinese), 10(1), 53-64, 1990.

Paronuzzi, P., Rigo, E., and Bolla, A.: Influence of filling–drawdown cycles of the Vajont reservoir on Mt. Toc slope stability, Geomorphology, 191, 75-93, 2013.

Pasquarè Mariotto, F. A., and Tibaldi, A.: Inversion kinematics at deep-seated gravity slope deformations revealed by trenching techniques, Nat. Hazards Earth Syst. Sci, 16, 663-674, 2016.

Pasquarè, F.A., Tormey, D., Vezzoli, L., Okrostsvaridze, A., and Tutberidze, B.: Mitigating the consequences of extreme events on strategic facilities: Evaluation of volcanic and seismic risk affecting the Caspian oil and gas pipelines in the Republic of Georgia, Journal of Environmental Management, 92, 1774-1782, 2011.

Pasuto, A., and Soldati, M.: Rock spreading. In: Dikau, R., Brunsden, D., Schrott, L., Visen, M.-L. (Eds.), Landslide recognition, Identification, movement and causes. Wiley, Chichester, 122-136, 1996.

Pinyol, N., Alonso, E., Corominas, J., and Moya J.: Canelles landslide: modelling rapid drawdown and fast potential sliding, Landslides, 9, 33–51, doi:10.1007/s10346-011-0264-x, 2012.

Nat. Hazards Earth Syst. Sci. Discuss., https://doi.org/10.5194/nhess-2018-186
Manuscript under review for journal Nat. Hazards Earth Syst. Sci.
Discussion started: 27 August 2018

Natural Hazards and Earth System Sciences
Open Access
Discussions

Radbruch-Hall, D.H.: Gravitational creep of rock masses on slopes, In: Voight, B. (Ed.), Rockslides and Avalanches, 1, Natural Phenomena, Developments in Geotechnical Engineering, 14A, 607-657, 1978.

Rebai, S., Philip, H., Dorbath, L., Borissoff, B., Haessler, H. and Cisternas, A.: Active tectonics in the Lesser Caucasus: coexistence of compressive and extensional structures, Tectonics, 12 (5), 1089–1114, 1993.

Reilinger, R.E., McClusky, S.C., Oral, M.B., King, R.W., Toksoz, M.N., Barka, A.A., Kinik, I., Lenk, O., and Sanli, I.: Global Positioning System measurements of present-day crustal movements in the Arabia-Africa-Eurasia plate collision zone, Journal of Geophysical Research, 102 (5), 9983–9999, 1997.

Reilinger, R.E., McClusky, S.C., Vernant, P., Lawrence, S., Ergintav, S., Cakmak, R., Ozener, H., Kadirov, F., Guliev, I., Stepanian, R., Nadariya, M., Hahubia, G., Mahmoud, S., Sakr, K., Arrajehi, A., Paradissis, D., Al-Aydrus, A., Prilepin, M., Guseva, T., Evren, E., Dmirotsa, A., Filikov, S. V., Gomez, F., Al-Ghazzi, R., and Karam, G.: GPS constraints on continental deformation in the Africa-Arabia-Eurasia continental collision zone and implications for the dynamics of plate interactions, Journal of Geophysical Research, 111(B5), doi: 10.1029/2005JB004051, 2006.

Schuster, R.L.: Reservoir-induced landslides, Bulletin of the International Association of Engineering Geology, 20, 8-15, 1979.

Schuster, R.L., and Wieczorek, G.F.: Landslide triggers and types, In: Rybar J., Stemberk J., Wagner P. (eds), Proc. 1st European Conference on Landslides, Prague, Czech Republic, Balkema Publishers, Taylor & Francis, Prague, 59–78, 2002.

Semenza, E., and Ghirotti, M.: History of the 1963 Vaiont slide: the importance of geological factors, Bulletin of Engineering Geology and the Environment, 59(2), 87-97, 2000.

Solonenko, V.P.: Landslides and collapses in seismic zones and their prediction, Bulletin of the International Association of Engineering Geology 15, 4–8, 1977.

Sosson, M., Rolland, Y., Danelian, T., Muller, C., Melkonyan, R., Adamia, S., Kangarli, T., Avagyan, A., and Galoyan, G.: Subductions, obduction and collision in the Lesser Caucasus (Armenia Azerbaijan, Georgia), new insights, In: Sosson, M., Kaymakci, N., Stephanson, R., Bergarat, F., Storatchenoko, V. (Eds.), Sedimentary Basin Tectonics from the Black Sea and Caucasus to the Arabian Platform, Geological Society of London Special Publication, 340, 329–352, 2010.

Tan, O., and Taymaz, T.: Active tectonic of the Caucasus: earthquake source mechanisms and rupture histories obtained from inversion of teleseismic body waves, Geological Society of America, special paper 409, 531-578, 2006.

Tibaldi, A., and Pasquarè, F.: Quaternary deformations along the 'Engadine–Gruf tectonic system', Swiss–Italian border, Journal of Quaternary Science, 23(5) 475–487, 2008.

Tibaldi, A., and Tsereteli, N.: International effort tackles landslide hazards to keep the peace, Eos, 98, doi:10.1029/2017EO065815. Published on 30 January 2017.

Nat. Hazards Earth Syst. Sci. Discuss., https://doi.org/10.5194/nhess-2018-186
Manuscript under review for journal Nat. Hazards Earth Syst. Sci.
Discussion started: 27 August 2018

Tibaldi, A., Ferrari, L., and Pasquarè, G.: Landslides triggered by earthquakes and their relationships with faults and mountain slope geometry: an example from Ecuador, Geomorphology, 11, 215-226, 1995.

Tibaldi, A., Rovida, A., and Corazzato C.: A giant deep-seated slope deformation in the Italian Alps studied by paleoseismological and morphometric techniques, Geomorphology, 58, 27–47, 2004.

Tibaldi, A., Corazzato, C., Rust, D., Bonali, F. L., Mariotto, F. P., Korzhenkov, A. M., Oppizzi P., and Bonzanigo, L.: Tectonic and gravity-induced deformation along the active Talas–Fergana Fault, Tien Shan, Kyrgyzstan, Tectonophysics, 657, 38-62, 2015.

Tibaldi, A., Alania, V., Bonali, F. L., Enukidze, O., Tsereteli, N., Kvavadze, N., and Varazanashvili, O.: Active inversion tectonics, simple shear folding and back-thrusting at Rioni Basin, Georgia, Journal of Structural Geology, 96, 35-53, 2017a.

Tibaldi, A., Russo, E., Bonali, F.L., Alania, V., Chabukiani, A., Enukidze, O., and Tsereteli, N.: 3-D anatomy of an active fault-propagation fold: a multidisciplinary case study from Tsaishi (Georgia), western Caucasus, Tectonophysics, 717, 253-269, 2017b.

Tsereteli, N., Tibaldi, A., Alania, V., Gventsadse, A., Enukidze, O., Varazanashvili, O., and Müller B.I.R.: Active tectonics of central-western Caucasus, Georgia, Tectonophysics, 691, B, 328-344, 2016.

Varazanashvili, O., Tsereteli, N., Bonali, F. L., Arabidze, V., Russo, E., Pasquarè Mariotto, F., Gogoladze, Z., Tibaldi, A., Kvavadze, N., and Oppizzi, P.: GeoInt: the first macroseismic intensity database for the Republic of Georgia, Journal of Seismology, 1-43, doi.org/10.1007/s10950-017-9726-5, 2018.

Varnes, D.J., Coe, J.A., Godt, J.W., Savage, W.Z., and Savage, J.E.: Measurement or ridge-spreading movements (sackungen) at Bald Eagle Mountain, Lake County, Colorado, II: continuation of the 1975–1989 measurements using a Global Positioning System in 1997 and 1999, U.S. Geological Survey, Open file report 00-205, on-line edition, 2000.

Varnes, D.J., Radbruch-Hall, D.H., and Savage, W.Z.: Topographic and structural conditions in areas of gravitational spreading of ridges in the western United States, U.S. Geological Survey Professional Paper, 1496, 28 pp, 1989.

Varnes, D.J., Radbruch-Hall, D.H., and Varnes, K.L.: Measurement of ridge spreading movements (sackungen) at Bald Eagle Mountain, Lake County, Colorado, 1975–1989, U.S. Geological Survey, Open File Report, 90-543, 13 pp, 1990.

Vincent, S.J., A. Carter, V.A. Lavrishchev, S.P. Price, T.G. Barabadze, and Hovius N.: The exhumation of the western Greater Caucasus: a thermochronometric study, Geological Magazine, 148, 1–21, 2011.

Vincent, S.J., Morton, A.C., Carter, A., Gibbs, S., and Teimuraz, G.B.: Oligocene uplift of the Western Greater Caucasus: An effect of initial Arabia-Eurasia collision, Terra Nova, 19, 160–166, 2007.

Zangerl, C., Eberhartd, E., and Perzlmaier, S.: Kinematic behaviour and velocity characteristics of a complex deep-seated crystalline rockslide system in relation to its interaction with a dam reservoir, Engineering Geology, 112, 53-67, 2010.

Zare, M., Amini, H., Yazdi, P., Sesetyan, K., Demircioglu, M.B., Kalafat, D., Erdik, M., Giardini, D., Khan, M.A., and Tsereteli N.: Recent developments of the Middle East catalog, Journal of Seismology, 18, N4, 749-772, DOI 10.1007/s10950-014-9444-1, 2014.

Zare, M., Amini, H., Yazdi, P., Sesetyan, K., Demircioglu, M.B., Kalafat, D., Erdik, M., Giardini, D., Khan, M.A., and Tsereteli, N.: Reply to "comment on 'recent developments of the Middle East catalog', Journal of Seismology, 21, 1, 269-271, 2017.

Zolotarev, G.S., Makhorin, A.A., and Federenko, V.S.: Geological map of left bank of river Enguri, upper part of Enguri HPP, Scale 1:2500, Ministry of Energy, CCCP, 1968.

Zhu, D., Yan, E., Hu, G., and Lin, Y.: Revival deformation mechanism of Hefeng Landslide in the Three Gorges Reservoir based on FLAC3D software, Procedia Engineering, 15, 2847-2851, 2011.